Journal of Natural Gas Science and Engineering 64 (2019) 133–151

Contents lists available at ScienceDirect

Journal of Natural Gas Science and Engineering

journal homepage: www.elsevier.com/locate/jngse

Late Jurassic Arwa Member in south-eastern Al-Jawf sub-basin, NW Sabatayn Basin of Yemen: Geochemistry and basin modeling reveal shale-gas potential

Mohammed Hail Hakimi[a,*], Abdulwahab S. Alaug[a], Ibrahim M.J. Mohialdeen[b], Ali Y. Kahal[c], Hesham Abdulelah[d], Yousif Taha Hadad[e], Madyan M.A. Yahya[a,c]

[a] Geology Department, Faculty of Applied Science, Taiz University, 6803, Taiz, Yemen
[b] Department of Geology, College of Science, University of Sulaimani, Kurdistan, Iraq
[c] Geology and Geophysics Department, College of Science, King Saud University, Riyadh, Saudi Arabia
[d] Shale Gas Research Group (SGRG), Institute of Hydrocarbon Recovery, Faculty of Petroleum & Geoscience, Universiti Teknologi PETRONAS, Seri Iskandar, 32610, Malaysia
[e] Oil Exploration and Production Authority (OEPA), Ministry of Petroleum, HQ, Khartoum, Sudan

ARTICLE INFO

Keywords:
Arwa shale
Shale gas-potential
Secondary cracking
Geochemistry
Basin modeling
Al-Jawf sub-basin
Yemen

ABSTRACT

The current study evaluated the source rock characteristics, thickness, and lithology of the Late Jurassic Arwa Member to provide information about both conventional and unconventional resource systems in the Al-Jawf sub-basin. Three exploratory wells in the south-eastern portion of the Al-Jawf sub-basin were used for the source rock geochemistry and basin modeling study.

Results from the geochemical and basin modeling indicate that the Arwa Member is a self contained source-reservoir whose shales are considered as gas-prone source rocks, and have generated large amounts of thermogenic gas through secondary cracking of oils at high thermal maturity levels. The geochemical results reveal that the Arwa shales currently contain Type III and IV kerogen in a gas-window maturity stage and are shale-gas resources.

The basin models illustrate that the late Jurassic to early Miocene age was the peak-oil generation window of the Arwa shale source rock, with a transformation ratio (TR) of 10–85%. Most of the oil was expelled along micro-fractures caused by the pressure of oil generated within the Arwa shales, which was then trapped in the carbonate reservoir rocks within the Arwa Member itself. The oil retained in the Arwa carbonate rocks was partially and/or completely cracked into gas between the early Miocene and the present-day. This thermogenic gas was generated due to high thermal maturity caused by Tertiary volcanic rocks. Assuming a thickness of 360–1590 m and partial and/or complete cracking of retained oil to gas, the Arwa Shale Member could have a huge gas-generation potential.

1. Introduction

The Sabatayn Basin contains many oilfields which have been used to produce commercial hydrocarbons (Beydoun, 1989, 1991; Bosence, 1997). The Sabatayn Basin includes the Al-Jawf, Marib, and Hajar sub-basins, and the Shabwah depression (Fig. 1).

The Marib sub-basin has been thoroughly scrutinized over the last 20 years and has attracted several hydrocarbon exploration and development activities. These activities were concentrated on the Late Jurassic Madbi and Safer source rocks (Brannin et al., 1999; Csato et al., 2001; Alaug et al., 2011; Sachsenhofer et al., 2012; Hakimi and Abdullah, 2013a; 2013b; Hakimi et al., 2014; Hatem et al., 2016).

Currently several petroleum source rock geochemistry projects are being conducted to investigate the onshore petroleum potential of the Sabatayn Basin and to encourage hydrocarbon exploration in order to improve knowledge about the conventional and unconventional reserves in the basin.

The Al-Jawf sub-basin belongs to the north-western part of the Sabatayn Basin (Fig. 2A). Limited hydrocarbon exploration started in the sub-basin in 1981 and seven exploratory wells (Fig. 2B) have been drilled by the Hunt Oil Company. This drilling has revealed the presence of oil and gas (SPT, 1994), which encouraged further study of the

* Corresponding author.
E-mail address: ibnalhakimi@yahoo.com (M.H. Hakimi).

https://doi.org/10.1016/j.jngse.2019.01.022
Received 26 October 2018; Received in revised form 30 January 2019; Accepted 31 January 2019
Available online 08 February 2019
1875-5100/

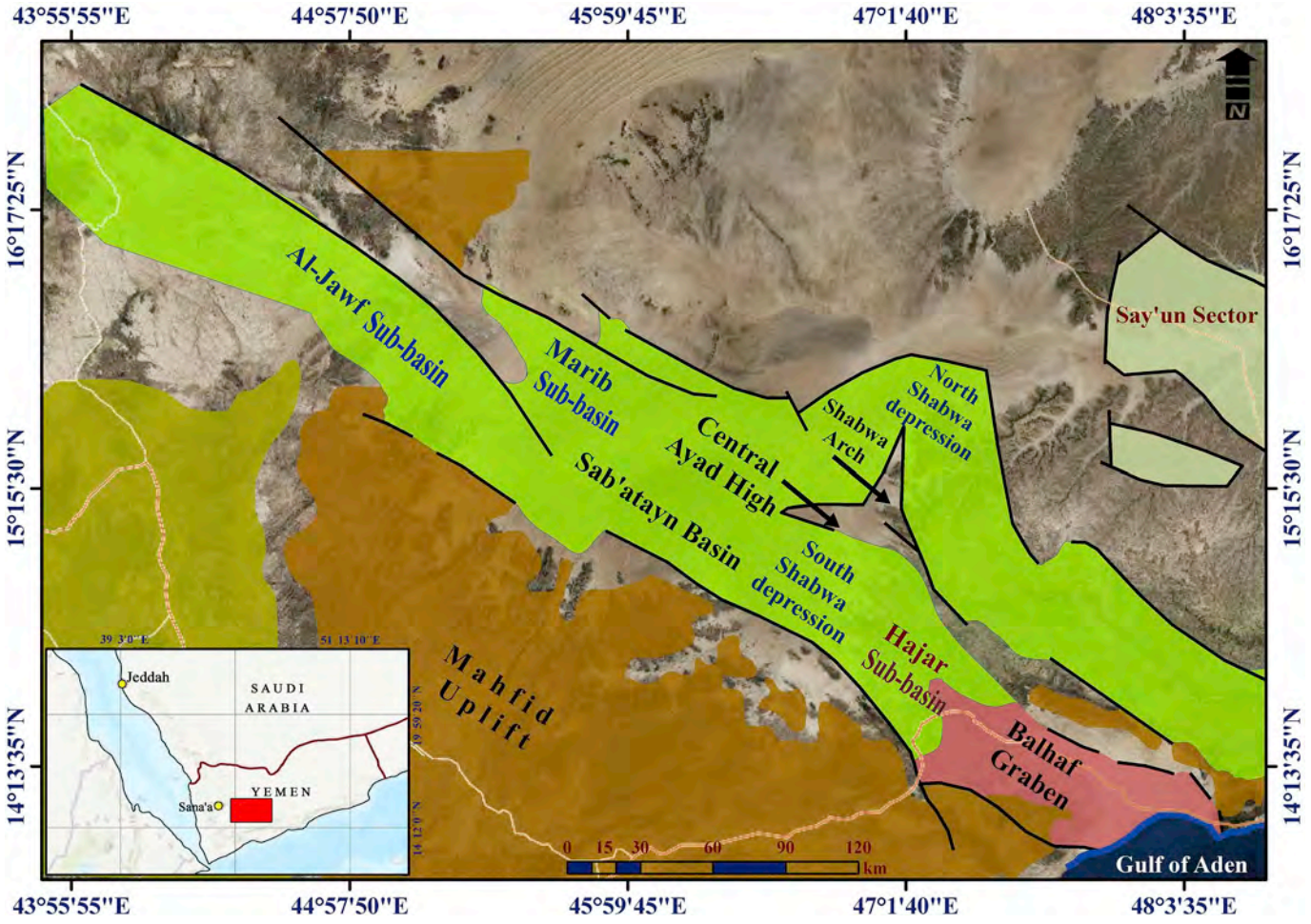

Fig. 1. Map of the Sabatyen Basin, showing several sub-basins (i.e. Al-Jawf, Marib and Hajar), and Shabwah depression (modified after Al-Areeq et al., 2018).

potential for petroleum resources along the Al-Jawf sub-basin. Potential source rocks from the Late Jurassic sedimentary rocks in the Al-Jawf sub-basin and the potential presence of petroleum has not been well studied and requires further research.

Organic matter has been discovered within the shale intervals of the Late Jurassic formations of the Al-Jawf sub-basin (Alaug and Al-Wosabi, 2015). The Late Jurassic (Kimmeridgian-Tithonian) Madbi shales, represented in several wells along the Al-Jawf sub-basin, are considered to be good source rocks for oil and gas generation, as reported by Alaug and Al-Wosabi (2015). Hence shale intervals within the entire late Jurassic succession were intensively investigated for petroleum generation potential in the Al-Jawf sub-basin.

As part of the petroleum geochemistry research, source rock evaluation and hydrocarbon generation potential for the underexplored Al-Jawf sub-basin has been investigated in the current study. The shale intervals within the Late Jurassic Arwa Member were analyzed for investigation into the source rock potential and petroleum generation in the south-eastern part of Al-Jawf sub-basin (Fig. 2B). This study was conducted parallel to studies considering source rock characterization and petroleum generation potential of the Late Jurassic Madbi Formation in the Al-Jawf sub-basin (Alaug and Al-Wosabi, 2015).

The main objective of this study was to document and quantify the organic matter, characterize kerogen type and quality, investigate the thermal maturity, and discern the hydrocarbon generation potential of the shale intervals within the Late Jurassic Arwa Member from three wells (Saba-01, Dahmar Ali −01, and Kamaran-01) in the south-eastern part of the Al-Jawf sub-basin (Fig. 2B). Additionally, basin modeling was incorporated to simulate the geothermal history and the timing of hydrocarbon generation of the potential source rocks in the region. The results of this study are expected to provide guidance for further exploration along the Al-Jawf sub-basin and an estimation of the conventional and unconventional reserves in the Sabatayn Basin.

2. Geological setting

The Sabatayn Basin is in northern central Yemen and is divided into several sub-basins (e.g. Al-Jawf, Marib and Hajar) and the Shabwah depression (Fig. 1). The onshore basins, including Sabatayn and Sayun-Masilah, were generated as rift basins associated with the Mesozoic disintegration of Gondwana during the late Jurassic-early Cretaceous (Redfern and Jones, 1995; As-Saruri et al., 2010). These tectonic events are manifested in normal faults that are associated with the extensional tectonics that have affected the basin since this period (Fig. 3).

The Al-Jawf-Marib sub-basins are filled with lower Palaeozoic (Cambrian-Permian) to Mesozoic (Jurassic-late Cretaceous) successions punctuated by unconformities of different magnitudes and ages (SPT,

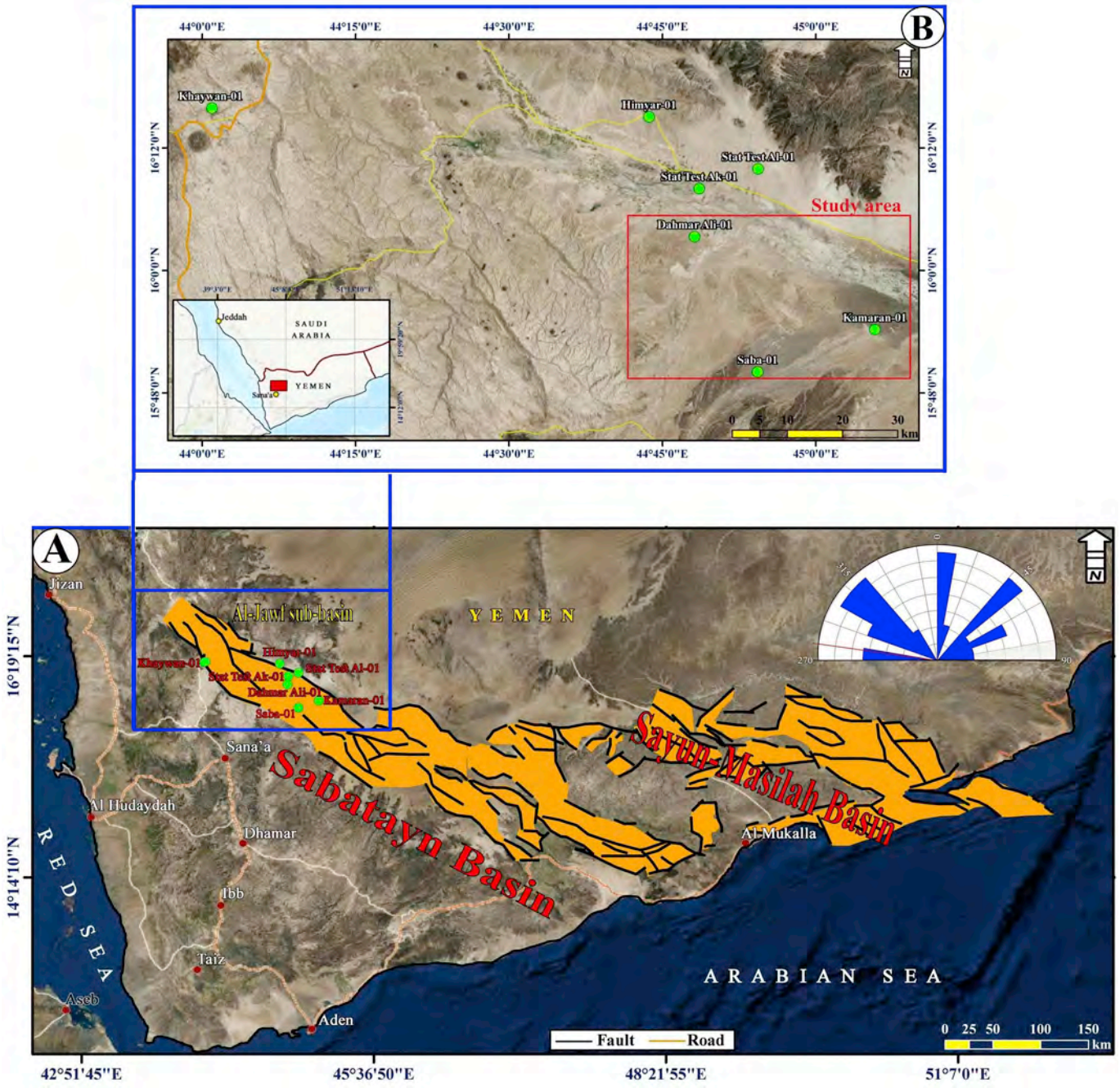

Fig. 2. (a) Main producing onshore sedimentary basins in Republic of Yemen, and (b) location map of the exploration wells in Al-Jawf sub-basin, NW Sabatayn Basin.

1994; As-Saruri et al., 2010; Alaug and Al-Wosabi, 2015). The lower Palaeozoic sedimentary sequence is represented by the Wajid and Akbra formations that lie unconformably on Precambrian basement rocks (Fig. 4). The Wajid Formation is characterized by continental sandstones and interbedded mudstones from the Cambrian–Carboniferous age (SPT, 1994; Beydoun et al., 1998; As-Saruri et al., 2010), while the Akbra Formation represents glacial deposits from the Permianice age (Beydoun et al., 1998; As-Saruri et al., 2010).

The Mesozoic deposits are dominated by marine carbonates, shales, and sandstones with evaporite intervals which are mainly related to syn-rift and post-rift tectono-stratigraphic phases (Fig. 4). Four sedimentary formations were deposited in the basin during the Jurassic period, from base to top namely: the Kuhlan Formation, the Shuqra Formation, the Madbi Formation and the Sabatayn Formation (Fig. 4). The Early-Middle Jurassic Kuhlan Formation is represented by continental to marine sandstones which vertically grade upwards into the carbonates of the Shuqra Formation (Beydoun et al., 1998; Al-Wosabi, and Al-Mashaikie, 2006). The overlying Shuqra Formation is composed of marine shales and carbonates divided into two members with a conformable contact (SPT, 1994), from base to top namely Saba and

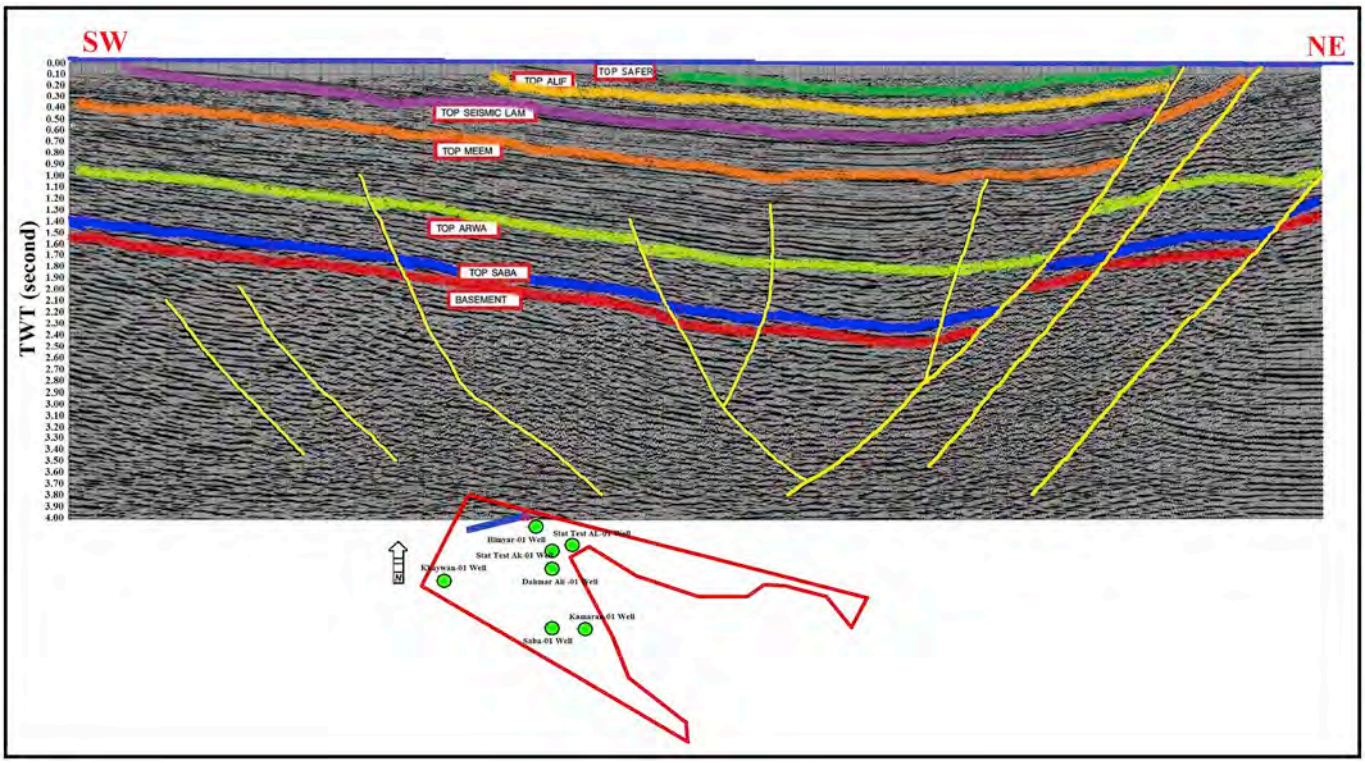

Fig. 3. Seismic section for one line (blue line) alone the exploratory wells, showing the primary structural setting and stratigraphic succession across the Al-Jawf sub-basin.

Arwa (Fig. 4). Based on the distribution of lithofacies of the Shuqra Formation, a neritic marine depositional environment was suggested (SPT, 1994; Beydoun et al., 1998). The upper part of the Shuqra Formation is comprised of marine-lime mudstone and the shale interbeds of the Arwa Member (Fig. 4), becoming clastic dominated towards the base (SPT, 1994). The Arwa member contains rich microspore assemblages, with abundant *Deltoidospors* spp., *Dictyophyllidites* spp., *Cupressacites oxycedroides* and *Exesipollenites* spp. (SPT, 1994). Based on the moderately diverse dinocyst assemblages including *Systematophora* spp., *Cribroperidinium* spp. and *Sentusidinium* spp. (SPT, 1994), a mid-Kimmeridgian age was suggested (SPT, 1994). For this study, shale samples were collected from the Arwa Member in the southeast portion of the Al-Jawf-Marib sub-basin (Fig. 1B), where the thickness of the Arwa deposit varies over different locations, with a total thickness of > 1500 m in the Dahmar Ali −01 well and about 400 m in the Saba-01 Well (Table 1). The Arwa Member was followed by the mixed limestones, shales and sandstones of the syn-rife Madbi Formation (Fig. 4). The Madbi Formation is divided into three members, from base to top namely Meem, Lam and Reydan (Fig. 4). The Meem and Lam members consist of shale, calcareous shale, and limestone interbedded with sandstone sediments (Fig. 4), while the Reydan member is mainly made up of sandstones (Fig. 4). Based on geochemical data from the Meem and Lam Madbi shales, it has been documented that the shales in the Sabatayn Basin are oil-prone source rocks (Brannin et al., 1999; Csato et al., 2001; Alaug et al., 2011; Hakimi et al., 2014; Alaug and Al-Wosabi, 2015; Al-Areeq et al., 2018). The Madbi Formation is conformably overlain by the mixed evaporite-clastic sequence of the late Tithonian Sabatayn Formation (Fig. 4). It has been observed that the thickness of the salt sediment accumulation changed during the Late Jurassic in the Sabatyen Basin, decreasing from the south-east portion (the Shabwah depression and Hajar sub-basin) to the north-western portion of the Sabatayn Basin (north Al-Jawf graben) (SPT, 1994). Mixed carbonate and shale deposits from the Late Jurassic-Early Cretaceous Azal Formation succeed the Sabatayn Formation with a conformable contact (Fig. 4), along with unconformably overlying Cretaceous (Aptian- Maastrichtian) sediments. Most of the Valanginian-Barremian age was a time of erosion and non-deposition (Fig. 4). The Valanginian-Barremian erosional vacuity event was followed by a sea level rise and the accumulation of the thick sandstone lithofacies of the Tawilah Group (Fig. 4).

Moreover, volcanic or sealed magmatic plutons are present in the wells (Saba-01, Dahmar Ali −01 and Kamaran-01), which have intruded into the older sedimentary rocks (Madbi Formation) as recognized during drilling processes (SPT, 1994). These volcanic rocks were formed during the middle to late Miocene as a result of Red Sea rifting (Al Kadasi, 1994; Nasher, 2010). The volcanic rocks or sealed magmatic plutons acted as a heat source to affect the thermal maturity level of the organic matter in the surrounding sedimentary rock (e.g., Zhu et al., 2007; Alalade and Tyson, 2013; Hakimi et al., 2017).

3. Material and methods

3.1. Samples and experimental methods

Ninety-one cutting shale and calcareous shale samples were collected from three exploration wells (Saba-01, Dahmar Ali −01 and Kamaran-01) in the south-eastern part of the Al-Jawf sub-basin (Fig. 2B). The samples were collected from the Arwa Member at 1054–1417 m, 2351–3914 m, and 3011–3711 m in the Saba-01, Dahmar Ali-01, and Kamaran-01 wells, respectively (Table 1).

The samples were analyzed at Simon Petroleum Technology Limited Laboratories in the United Kingdom and subjected to conventional

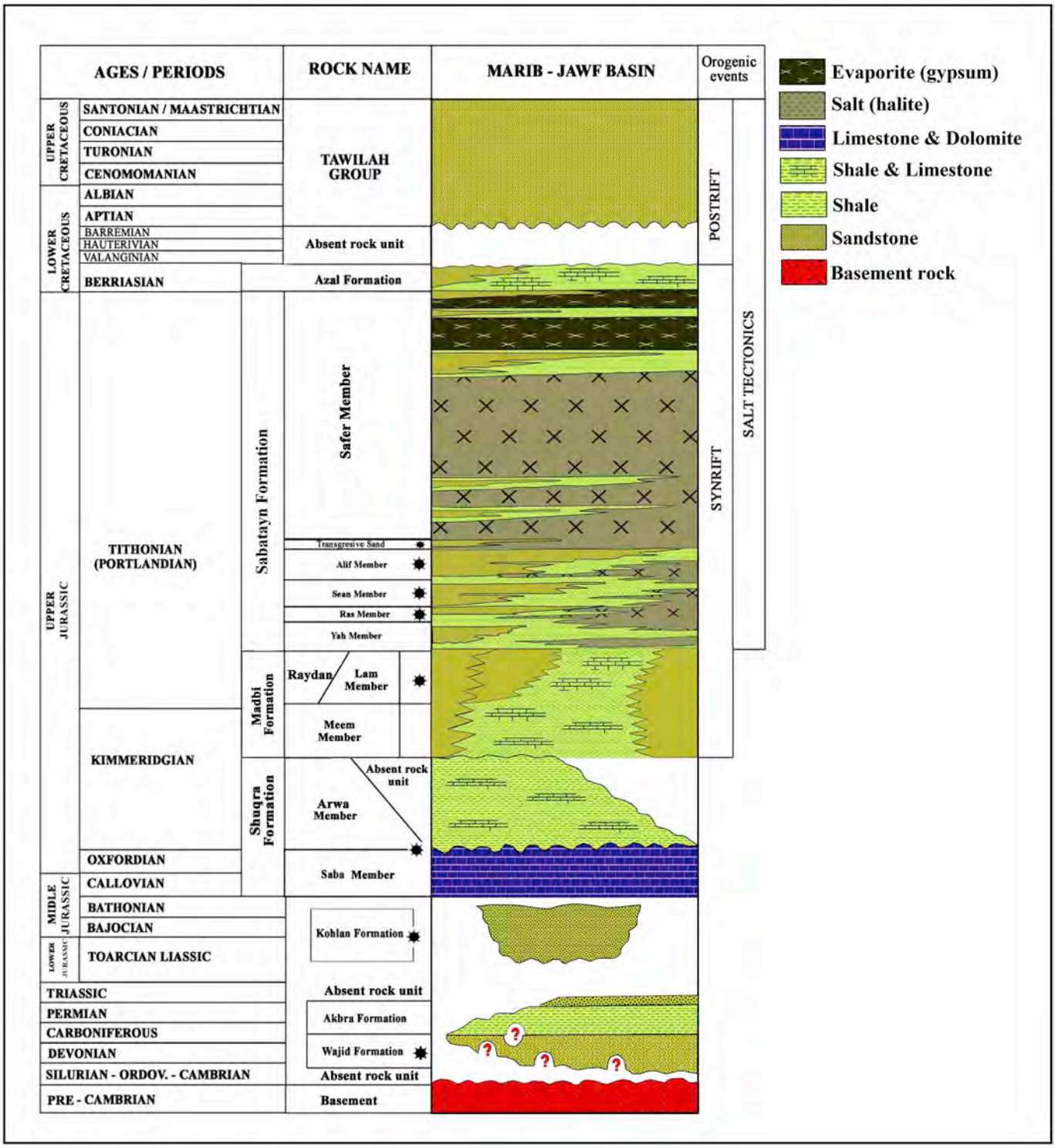

Fig. 4. Generalized stratigraphic column of Palaeozoic sections (Cambrian-Permian) followed by a thick Mesozoic succession (Jurassic-Cretaceous) in Marib-Al-Jawf basin.

source rock geochemistry analyses such as total organic carbon (TOC) content and Rock-Eval pyrolysis as well as vitrinite reflectance (VR) measurements under reflected microscopy light. The basic geochemical and VR analyses of the target stratum were used to investigate the possible conventional and unconventional resources of the potential source rocks within the Al-Jawf sub-basin.

A total of 91 samples were crushed into powder and pre-treated with concentrated HCl to remove carbonates for TOC measurement.

Table 1
Basin model input data used to reconstruct the burial history for three well locations (Saba-01, Dahmar Ali −01 and Kamaran-01) in the south-eastern Jawf sub-basin, NW Sabatyen Basin, Yemen.

Dahmar Ali −01 Well											
Tectonic	Formations/Members		Top	Bottom	Thickness	Lithology	Deposition ages		Erosion age		Erosion Thickness
							From	To	From	To	
Syn-rift	Lam Member	Madbi Formation	46	1441	1395	Sandstone &Limestone & Shale	150.8	149.6			
	Meem Member		1441	2351	910	Shale	156.3	150.8			
Pre-rift	Arwa Member		2351	3944	1593	Shale & Limestone	157.9	156.3	162.5	157.9	300
	Kuhlan Formation		3944	3972	28	Sandstone	167.7	162.5			
Total depth			**3972**			–	–	–	–	–	–
Kamaran-01 Well											
Tectonic	**Formations/Members**		**Top**	**Bottom**	**Thickness**	**Lithology**	**Deposition ages**		**Erosion age**		**Erosion Thickness**
							From	**To**	**From**	**To**	
Post-rift	Tawilah Formation		45	442	397	Sandstone	142.9	112			
Syn-rift	Azal Formation		442	501	59	Limestone & Shale	148.5	142.9			
	Sabatyen Formation		501	869	368	Sandstone & Shale & evaporite	149.6	148.5			
	Lam Member	Madbi Formation	869	2275	1406	Sandstone &Limestone & Shale	150.8	149.6			
	Meem Member		2275	3011	736	Shale	156.3	150.8			
Pre-rift	Arwa Member	Shuqra Formation	3011	3711	700	Shale & Limestone	157.9	156.3			
	Saba Member		3711	4179	468	Limestone & Shale	162.5	157.9			
Total depth			**4179**			–	–	–	–	–	–
Saba-01 Well											
Tectonic	**Formations/Members**		**Top**	**Bottom**	**Thickness**	**Lithology**	**Deposition ages**		**Erosion age**		**Erosion Thickness**
							From	**From**	**From**		
Syn-rift	**Lam Member**	**Madbi Formation**	30	549	519	Sandstone & Shale	150.8	149.6			
	Meem Member		549	1054	505	Shale &Limestone	156.3	150.8			
Pre-rift	**Arwa Member**	**Shuqra Formation**	1054	1417	363	Shale &Limestone	157.9	156.3			
	Saba Member		1417	1555	138	Limestone	162.5	157.9			
	Kuhlan Formation		1555	1567	12	Sandstone	167.7	162.5			
	Total depth		**1567**			–	–	–	–	–	–

The pre-treated samples were then analyzed using a LECO CS125 instrument. Of these, 37 samples were used for pyrolysis analysis by referring to the Rock-Eval pyrolysis evaluation standard. The pyrolysis workstation was conducted on a Rock Eval-II instrument. In the Rock Eval-II instrument, S_1 (free hydrocarbon, mg/g), S_2 (total hydrocarbon amount from kerogen pyrolysis, mg/g), and T_{max} (maximum peak, °C) were obtained (Table 2). The Hydrogen Index (HI= S_2X100/TOC, mg HC/g TOC) and Production Index [PI=$S_1/(S_1+S_2)$] were subsequently calculated (Table 2).

Vitrinite reflectance analysis was performed on material from the Late Jurassic to Early Cretaceous stratigraphic levels at the three well locations (Kamaran-01, Dahmar Ali-01, and Saba-01), and used to predict past thermal conditions. For the analyzed Arwa Member, several samples from each well (7 samples from Kamaran-01, 7 samples from Dahmar Ali-01 and 4 samples from Saba-01) were selected for VR analysis.

The VR analysis was carried out on polished blocks of whole rock samples and performed under reflected white light through a 50× magnification oil immersion objective lens, using a Zeiss microscope. Measurements of the VR, expressed as %VRo, were deciphered using an interactive computer program which allows the operator to select, calculate, and plot population and mean reflectance.

3.2. Basin modeling procedure

In this study, three exploration wells (Kamaran-01, Dahmar Ali-01, and Saba-01) located within in the south-eastern part of the Al-Jawf sub-basin (Fig. 2B) were used as representative sites to simulate the petroleum generation and expulsion history of the Arwa potential source rock. The burial and thermal history was reconstructed using the PetroMod 1D software (version 2010 SP1) of Schlumberger.

The thermal maturity history of the study area was reconstructed by integrating geological and geochemical data from the three wells. The thermal history and paleo-heat flow evolution of the sedimentary basins was estimated using thermal maturity calibration data such as vitrinite reflectance (VR) and bottom hole temperature (BHT) (Table 3).

Geological data such as lithology and periods of deposition and erosion, with associated ages (Table 1), are also required as basin modeling data input to reconstruct the subsidence and burial history of the region and to establish the burial and thermal history of the potential source rocks. Geochemical data such as the mean values of %TOC and HI, as well as kinetic models, are required to compute petroleum generation and expulsion throughout the corresponding geological age (Hakimi et al., 2010; Shalaby et al., 2011, 2013; Abeed et al., 2013; Hakimi and Abdullah, 2015; Makeen et al., 2016; Hadad et al.,

2016, 2017). Mean TOC and HI values of more than 1% and 450 mg HC/g TOC, respectively, were used in this study for low maturity samples of Arwa source rock (Hakimi et al., 2018). Hakimi et al. (2018) indicated that the Arwa shale samples in the shallow wells have original HI values of more than 400 mg HC/g TOC. The kinetic data produced by Tissot et al. (1987) for Type II kerogen using the PetroMod software is consistent with the source rock properties of the analyzed Arwa Shale Member. Therefore, these results were used as the default kinetic data to simulate petroleum generation and expulsion from the analyzed Arwa shale source rock.

4. Results and discussion

4.1. Organic matter content and hydrocarbon generative potential

Organic matter richness is a critical index used to evaluate the hydrocarbon generation ability of source rocks (Huang et al., 2010). The extent of organic matter content is usually evaluated as the TOC content in wt% (Peters and Cassa, 1994; Hunt, 1996). It has been suggested that a TOC content of 1.0 or more indicates an organic carbon content favorable for hydrocarbon generation (Peters and Cassa, 1994; Hunt, 1996). The analyzed shale samples were therefore classified as having a fair to good source generation potential, with TOC values of between 0.46% and 3.02% (Mean = 1.14%). While the majority of the analyzed samples had a TOC of between less than 1% and approximately 1%, six samples had relatively high TOC values of more than 2% (Table 2).

The S_2 hydrocarbon, generated during pyrolysis, is also a useful parameter for evaluating the hydrocarbon generation potential of source rocks (Peters, 1986; Bordenave, 1993). The hydrocarbon (S_2) yield of the analyzed samples ranged from 0.12 to 1.39 mg/g (Table 2). Based on these results, it can be said that the shales of the Arwa Member have a poor to fair hydrocarbon generation potential in the present-day (Fig. 6). However, this could be attributed to thermal maturity (see maturity section). The poor hydrocarbon generation potential of the analyzed samples could also suggest that the analyzed samples may have exhausted any potential hydrocarbons, as indicated by the presence of non-indigenous materials (migrated HCs) in the analyzed samples (Fig. 7).

Table 2
Geochemical results of the analyzed shale samples within Late Jurassic Arwa Member from three wells (Saba-01, Dahmar Ali −01 and Kamaran-01) in the southeastern Jawf sub-basin, NW Sabatyen Basin, Yemen, including TOC content and measured and calculated Rock-Eval pyrolysis parameters.

Wells	Depths (m)	TOC Wt.%	Rock-Eval pyrolysis data				
			S_1 (mg/g)	S_2 (mg/g)	HI (mg/g)	PI (mg/g)	T_{max} (°C)
Saba -01	1064	0.65	0.23	0.45	69	0.34	437
	1091	1.11	0.48	0.93	84	0.34	449
	1100	1.01	–	–	–	–	–
	1109	1.31	–	–	–	–	–
	1119	2.56	–	–	–	–	–
	1183	0.46	0.12	0.12	26	0.50	435
	1201	1.31	0.76	1.03	79	0.42	457
	1202	1.81	1.15	1.18	65	0.49	462
	1277	0.81	0.34	0.36	44	0.49	451
	1305	0.91	0.33	0.37	41	0.47	460
	1308	1.42	0.45	0.50	35	0.48	469
	1369	1.44	0.48	0.73	51	0.40	468
	1378	1.45	–	–	–	–	–
	1381	1.51	0.46	0.60	40	0.43	471
	1383	1.60	–	–	–	–	–
	1390	1.54	–	–	–	–	–
	1390	2.30	0.44	0.62	27	0.41	470
	1402	3.02	0.77	1.39	46	0.36	468
	1407	2.19	0.38	0.35	16	0.52	470
	1408	1.81	0.27	0.27	15	0.50	422
Dahmar Ali -01	2353	0.72	–	–	–	–	–
	2426	0.67	0.18	0.29	43	0.38	441
	2545	1.09	0.24	0.46	42	0.34	456
	2554	0.82	–	–	–	–	–
	2591	1.02	0.50	0.40	39	0.56	455
	2637	1.46	0.10	0.12	8	0.45	457
	2774	0.59	0.23	0.33	56	0.41	461
	2893	0.64	0.23	0.25	39	0.48	461
	2911	0.75	–	–	–	–	–
	3176	0.63	0.33	0.24	38	0.58	454
	3185	0.87	–	–	–	–	–
	3359	0.95	1.04	0.32	34	0.76	419
	3368	0.80	–	–	–	–	–
	3423	0.51	0.53	0.23	45	0.70	430
	3441	0.75	–	–	–	–	–
	3469	0.64	0.56	0.47	73	0.55	439
	3487	0.82	–	–	–	–	–
	3563	1.61	0.76	0.32	20	0.70	445
	3575	1.61	–	–	–	–	–
	3612	2.06	–	–	–	–	–
	3630	1.50	1.05	0.47	31	0.69	419
	3639	1.68	0.97	0.25	15	0.79	462
	3648	1.43	–	–	–	–	–

(continued on next page)

Table 2 (*continued*)

Wells	Depths (m)	TOC Wt.%	Rock-Eval pyrolysis data				
			S_1 (mg/g)	S_2 (mg/g)	HI (mg/g)	PI (mg/g)	T_{max} (°C)
Kamaran -01	2716	0.74	–	–	–	–	–
	2725	1.58	–	–	–	–	–
	2752	0.60	0.17	0.26	43	0.40	484
	2844	0.73	0.23	0.27	37	0.46	479
	2896	1.91	0.25	0.67	35	0.27	453
	2899	0.96	–	–	–	–	–
	2908	1.62	1.3	0.55	34	0.70	471
	2926	1.24	0.47	0.33	27	0.58	472
	2927	1.13	0.47	0.43	38	0.52	456
	2935	0.96	–	–	–	–	–
	2944	1.30	0.45	0.62	48	0.42	504
	2966	1.10	–	–	–	–	–
	2984	0.81	0.47	0.35	43	0.57	457
	3021	0.77	0.45	0.28	36	0.62	501
	3030	0.89	0.58	0.30	34	0.66	449
	3118	0.93	0.58	0.23	25	0.71	424
	3127	1.10	–	–	–	–	–
	3136	1.22	1.12	0.39	32	0.74	426
	3146	1.02	–	–	–	–	–
	3164	1.00	–	–	–	–	–
	3191	1.09	–	–	–	–	–
	3200	1.04	–	–	–	–	–
	3219	0.97	–	–	–	–	–
	3237	0.84	0.62	0.32	38	0.66	419
	3246	0.94	–	–	–	–	–
	3264	0.96	–	–	–	–	–
	3274	0.92	–	–	–	–	–
	3283	0.88	0.47	0.30	34	0.61	423
	3292	0.87	–	–	–	–	–
	3310	1.01	–	–	–	–	–
	3316	0.83	–	–	–	–	–
	3328	1.42	0.82	0.31	22	0.72	504
	3347	0.92	0.48	0.26	28	0.65	432
	3356	1.00	–	–	–	–	–
	3374	0.55	0.22	0.34	62	0.39	495
	3383	0.99	–	–	–	–	–
	3411	1.23	0.52	0.26	21	0.67	485
	3420	1.06	–	–	–	–	–
	3429	0.97	0.24	0.21	22	0.53	445
	3431	0.73	0.18	0.13	18	0.57	439
	3475	0.68	0.27	0.18	26	0.60	455
	3523	0.83	0.27	0.23	28	0.54	540
	3560	0.83	0.32	0.18	22	0.64	404
	3569	0.81	0.23	0.21	26	0.52	454
	3572	0.90	–	–	–	–	–
	3581	0.99	0.75	0.17	17	0.82	426
	3682	0.97	0.45	0.14	14	0.77	415
	3700	2.29	0.45	0.48	21	0.48	446

TOC: Total organic Carbon, wt% S_1: Volatile hydrocarbon (HC) content, mg HC/g rock PI: Production Index = $S_1/(S_1+S_2)$ S_2: Remaining HC generative potential, mg HC/g rock HI: Hydrogen Index = S_2x 100/TOC, mg HC/g TOC.

The migrated and indigenous hydrocarbons can be distinguished using the Rock-Eval pyrolysis data onS_1 and PI. According to Hunt (1996), the relatively high $S_1$and low TOC values are indicative of the presence of migrated hydrocarbons. Fig. 7A presents the plot of S_1 versus TOC values obtained in this study and indicates that the analyzed samples contained indigenous hydrocarbons together with a significant amount of migrated hydrocarbon. Additionally, the T_{max} values of less than 430 °C in several analyzed samples (Table 2) may be due to the presence of migrated hydrocarbons (Peters, 1986; Shalaby et al., 2012). The presence of migrated hydrocarbons in the analyzed samples conforms to PI values of more than 0.50 (Fig. 7B), since petroleum migration and expulsion can affect both S_1 and S_2 values (Abrams et al., 2017).

4.2. The quality of organic matter (remaining kerogen type)

The quality of the organic matter is an important criterion to evaluate the petroleum generation potential of a source rock (Peters and Cassa, 1994; Hunt, 1996; Zhang, 2012). The Rock-Eval HI value reflects the source and type of the organic matter (Peters and Cassa, 1994; Hunt, 1996; Liu et al., 2015). The relationship between Rock-Eval pyrolysis of T_{max} and HI values was used to identify the kerogen type in

Table 3
Vitrinite reflectance measurement of the Jurassic section including Arwa Member and corrected bottom whole temperatures at three studied wells (Saba-01, Dahmar Ali −01 and Kamaran-01) in the south-eastern Jawf sub-basin, NW Sabatyen Basin, Yemen.

Dahmar Ali −01 well				Kamaran-01 well				Saba-01 well			
Vitrinite Reflectance		Temperature		Vitrinite Reflectance		Temperature		Vitrinite Reflectance		Temperature	
Depth (m)	*VR_o (%)*	*Depth (m)*	*BHT (°C)*	*Depth (m)*	*VR_o (%)*	*Depth (m)*	*BHT (°C)*	*Depth (m)*	*VR_o (%)*	*Depth (m)*	*BHT (°C)*
334	0.37	931	70.6	394	0.34	547	49.4	73	0.54	1167	87.2
415	0.40	2227	112.8	405	0.30	1247	63.3	116	0.65	1198	87.8
492	0.39	3943	185.0	593	0.37	2414	111.1	210	0.62	1772	113.9
604	0.38	3986	163.9	828	0.42	2415	103.3	341	0.69		
714	0.38			882	0.49	4183	158.3	436	0.75		
890	0.40			893	0.50	4178	167.8	463	0.66		
989	0.42			924	0.50	4179	177.8	600	0.80		
1076	0.46			963	0.51			686	1.80		
1326	0.45			1001	0.52			701	2.25		
1472	0.55			1079	0.53			732	2.80		
1625	0.62			1098	0.56			934	2.50		
1734	0.75			1187	0.58			972	1.30		
1780	0.74			1205	0.59			1027	1.27		
2039	1.10			1245	0.59			1210	1.28		
2161	1.80			1292	0.57			1301	1.32		
2323	1.30			1342	0.58			1381	1.45		
2358	1.26			1381	0.60			1426	1.60		
2437	1.28			1440	0.61						
2658	1.20			1500	0.60						
2792	1.22			1561	0.68						
2914	1.22			1615	0.70						
3187	1.40			1920	0.75						
3307	1.60			2021	0.82						
3374	1.65			2155	0.87						
3435	1.90			2185	0.83						
				2244	0.83						
				2295	0.91						
				2332	0.88						
				2411	0.98						
				2454	1.27						
				2530	1.45						
				2595	1.38						
				2758	1.38						
				2913	1.50						
				3036	1.80						
				3078	1.80						
				3449	1.90						
				3574	1.80						
				3778	2.00						
				3850	2.10						

the analyzed samples.

Fig. 8 presents a cross plot of the present-day HI and T_{max} values and shows the remaining types of kerogen in the analyzed Arwa samples. In Fig. 8, the present-day kerogen types can be divided into two kinds: Type IV, with an HI value of less than 50 mg HC/g TOC; and Type III, with an HI value between 50 and 84 mg HC/g TOC. Most of the HI values were less than 50 mg HC/g TOC, indicating that the remaining kerogen mainly consists of Type IV kerogen (Fig. 8).

Fig. 8 also presents the relationship between T_{max} and kerogen type in terms of HI values. Based on the T_{max} values, the analyzed samples can be subdivided into two categories: the first is characterized by a T_{max} greater than 435 °C, which is of the mature to over-mature stage. The second is characterized by a T_{max} of below 435 °C, which points to the immature stage. T_{max} values of less than 435 °C could be due to the presence of migrated hydrocarbons within the analyzed samples, as indicated by S_1 and PI (Fig. 7). In contrast, T_{max} values greater than 435 °C indicate that the present-day kerogen (IV/III) in the analyzed samples is not original and the organic matter that accumulated during deposition was altered in the past due to thermal maturity.

4.3. The thermal maturity of organic matter

The evaluation of the thermal maturity of organic matter in a source rock mainly utilizes optical indicators, i.e. VR, spore coloration and geochemical parameters, i.e., Rock-Eval T_{max} and PI (Tissot and Welte, 1984; Sweeney and Burnham, 1990; Manning, 1991; Espitalie and Bordenave, 1993; Peters and Cassa, 1994; Hunt, 1996).

For this study, the evolution of the thermal maturity of the organic matter over this geological time was estimated using measured VR, Rock-Eval T_{max}, and PI data (Tables 2 and 3). VR has been widely used to measure the thermal maturity of organic matter under a microscope (Tissot and Welte, 1984; Sweeney and Burnham, 1990; Manning, 1991; Teichmüller et al., 1998; Killops and Killops, 2005). Fig. 9 shows the vertical cross-plot of VR distribution adjacent to the depths corresponding to the Late Jurassic to early Cretaceous sedimentary rocks throughout the three study wells. This cross-plot shows that the VR

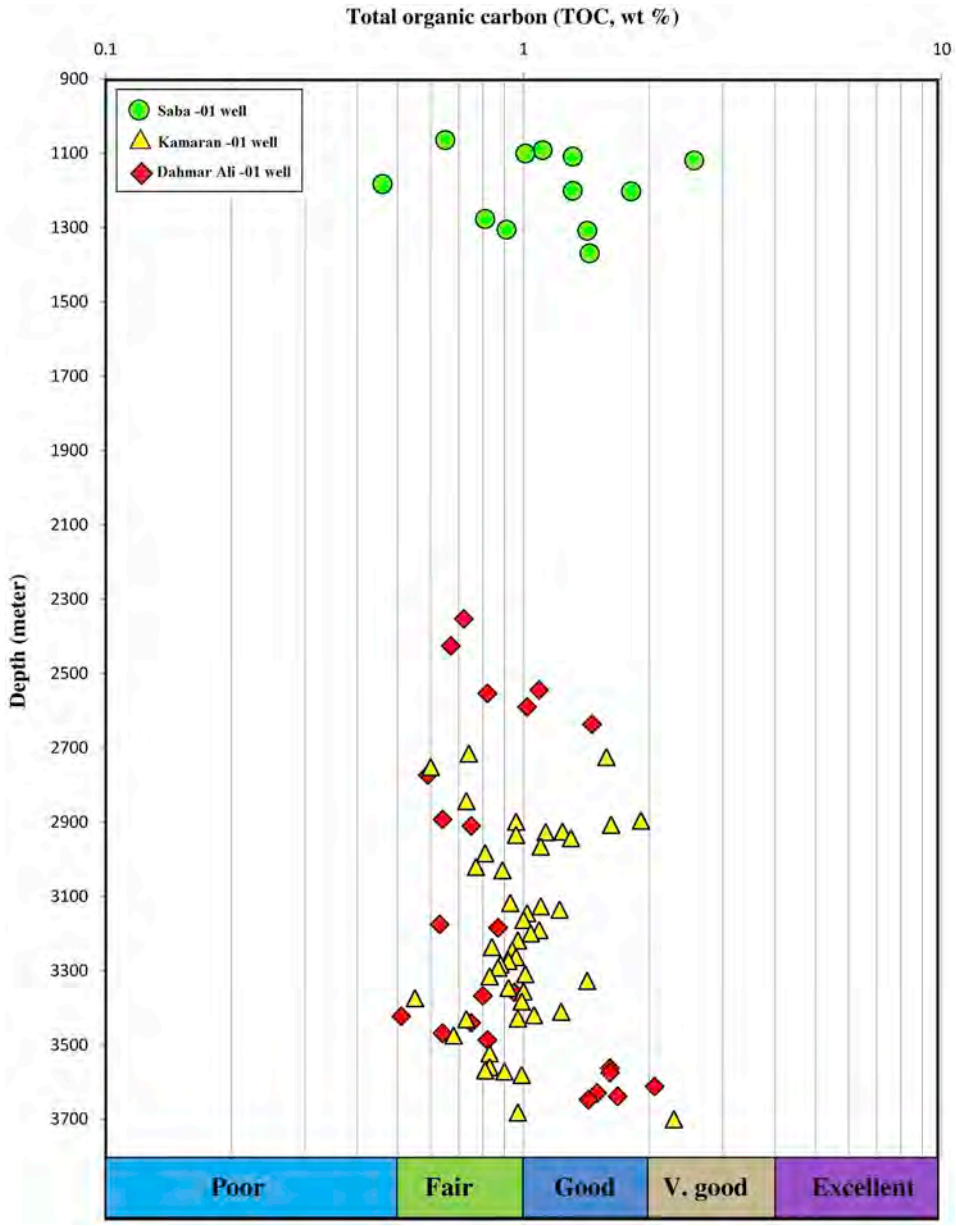

Fig. 5. Distribution of present-day total organic matter (TOC) content through depths of the analyzed Arwa samples from three studied wells in the south-eastern Al-Jawf sub-basin.

increased with burial depth (Fig. 9). However, VR values of less than 0.5% indicate an immature stage and the mature (oil-window) to over-mature (gas-window) stages correspond to VR values between 0.51% and 2.10% (Fig. 9). In the Kamaran-01 and Dahmar Ali-01 wells, the higher maturity is mainly due to both deeper burial and the presence of local volcanic rocks. The presence of the volcanic rocks (Fig. 9) alone explains the higher maturity in the other well (Saba-01), as reported by the oil company during the drilling process (SPT, 1994).

The apparent higher maturity level (1.28–2.1 VR%) of the studied Arwa Member from the three wells is consistent with gas-window generation (Fig. 9).

A map view of the mean VR measurements (VRo%) was prepared from the three studied wells (Kamaran-01, Dahmar Ali-01, and Saba-01) in the south-eastern portion of the Al-Jawf sub-basin, and wells from two locations (Himyar-01 and Khaywan-01) in the north-western and northern portions (Fig. 10). This map was used to discuss the different thermal maturity distribution of organic matter in the Arwa Shale and its relevance to hydrocarbon generation along the Al-Jawf sub-basin. The map indicates that the Late Jurassic Arwa Member is at immature to early-mature stages in the north-western and northern portions of the Al-Jawf sub-basin, and that the south-eastern portion has reached high maturity (Fig. 10). Therefore, the Arwa Member was not considered for commercial oil-generation in the north-western and north portions, while the south-eastern portion can be considered as a potential hydrocarbon (gas-window) region (Fig. 10).

The high thermal maturity levels of the organic matter in the analyzed Arwa samples were also observed using other geochemical maturity indicators. According to the Rock-Eval results, most analyzed

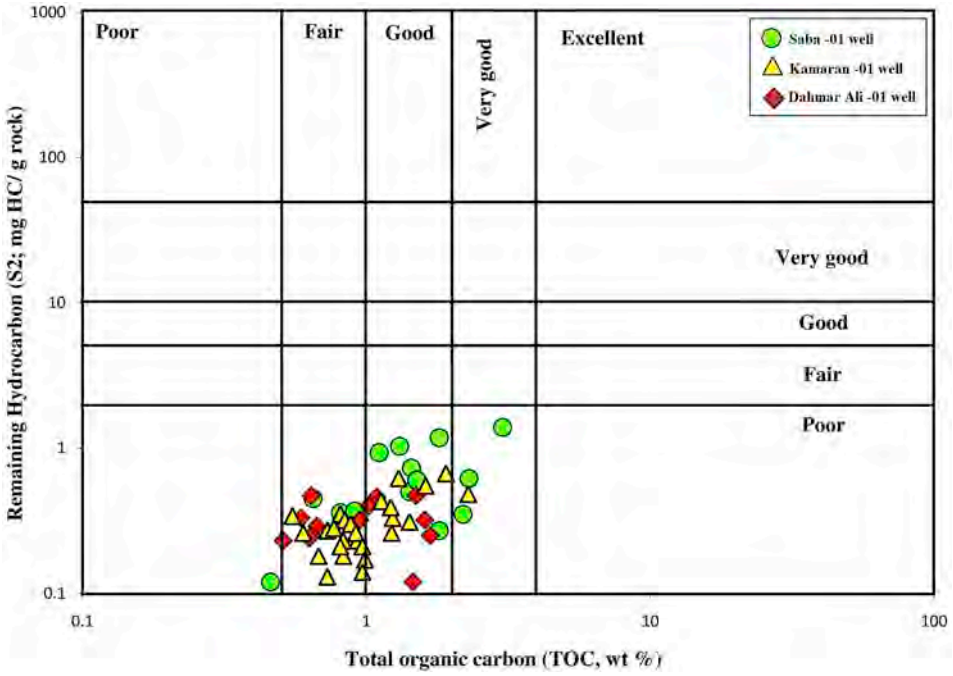

Fig. 6. Relationship between present-day total organic matter (TOC) content and remaining petroleum yield (S_2) for the analyzed Arwa samples from three studied wells.

samples had T_{max} values between 450 and 540 °C (Table 2) indicating the high thermal maturity levels (Fig. 8) that are usually found within oil, condensate, and dry-gas zones (Fig. 7B).

4.4. Petroleum generation evolution

The evolution of petroleum generation in the analyzed Late Jurassic Arwa Member during thermal maturation has been discussed in this study. The results of this study reveal a source rock characterization of the Arwa Member Shale samples. The analyzed Arwa samples that contain Types III/IV kerogen (Fig. 8) would mainly generate gas (Fig. 11). According to both optical (i.e. VRo%) and geochemical (i.e. T_{max} and PI) maturity data, the analyzed Arwa Shale in the study area has reached the gas-window generation stage (Fig. 9). The efficient thermal maturity of the analyzed Arwa Member depends on two factors; burial depth and the presence of local sill volcanic rocks (Fig. 9; SPT, 1994). However, the high thermal maturity affected the HI values and petroleum generation potential of the source rocks, decreasing both. Therefore, the current kerogen types reflect the present-day generation potential.

The original petroleum generation potential corresponding to kerogen type was estimated based on the quantitative mean of the original HIoriginal of the source rock (Jarvie et al., 2007). The average value of HIoriginal can be calculated from the percentages of the four kerogen types found in low maturity source rock samples. The average HIoriginal was calculated from different kerogen types derived from a range of HI values as per Jones (1984):

HIoriginal = (%Type I/100*750) + (%Type II/100*450) + (%Type III/100*125) + (%Type IV/100*50)

The mostly un explored areas of the north and the north-western portions of the Al-Jawf sub-basin contain Arwa samples that are at thermally immature to early-mature stages (Fig. 10). Hence, it was straightforward to determine the HIoriginal values. Hakimi et al. (2018) concluded that low maturity Arwa samples in the Khyawan-01 and Himyar-01 wells (Fig. 10) containhigh amounts of oil-liptinitic organic matter (Type I/II kerogens) followed by low amounts of Type III kerogen as shown in Fig. 12. Applying the above equation (Jones, 1984) to visual kerogen types from low maturity samples, the average calculated value of HIoriginal was found to be 482 mg/g TOC. This is a typical Type II kerogen and indicative of oil-source generation potential in the Arwa Member Shale.

Based on the current state of thermal maturity (average 1.60 VRo) and the original generation potential (Type II), it can be concluded that the bitumen has decomposed to oil and then the oil cracked to gas. Therefore, the Arwa Member Shale in the south-eastern part of the Al-Jawf sub-basinappears to be a potential shale-gas source.

4.5. Gas generation

The gas within the shale can be formed by three distinct processes: the conversion of kerogen to gas and bitumen, the conversion of bitumen to oil and gas due to primary cracking, and the cracking of retained oil to gas and pyrobitumen as a secondary process (Jarvie et al., 2007, Fig. 13). The secondary cracking depends on the retention of generated oil in the source rock system, which is a key to its gas potential (Jarvie et al., 2007).

In the oil-prone Type II kerogen, the gas is generated by the cracking of retained oil at high thermal maturity levels (Lewan and Henry, 2001). According to previous work, the analyzed Arwa Shale Member was considered to be a Type II oil-prone source rock in the north-western and northern portions of the Al-Jawf sub-basin (Hakimi et al., 2018). However, the results of this study suggest that the Arwa Shale Member in the south-eastern Al-Jawf sub-basin has a high gas potential due to the cracking of oil at higher thermal maturity levels. Therefore, the generation of gas from an oil-source rock through the cracking of generated oil was modelled.

Based on results from the modeling of the Arwa Shale Member, the cracking ofprimary kerogen to oil was found to occur between the temperatures of 80 and 152 °C (Fig. 14),corresponding to the computed VR values of between 0.70%Ro and 1.30%Ro, respectively (Fig. 15),

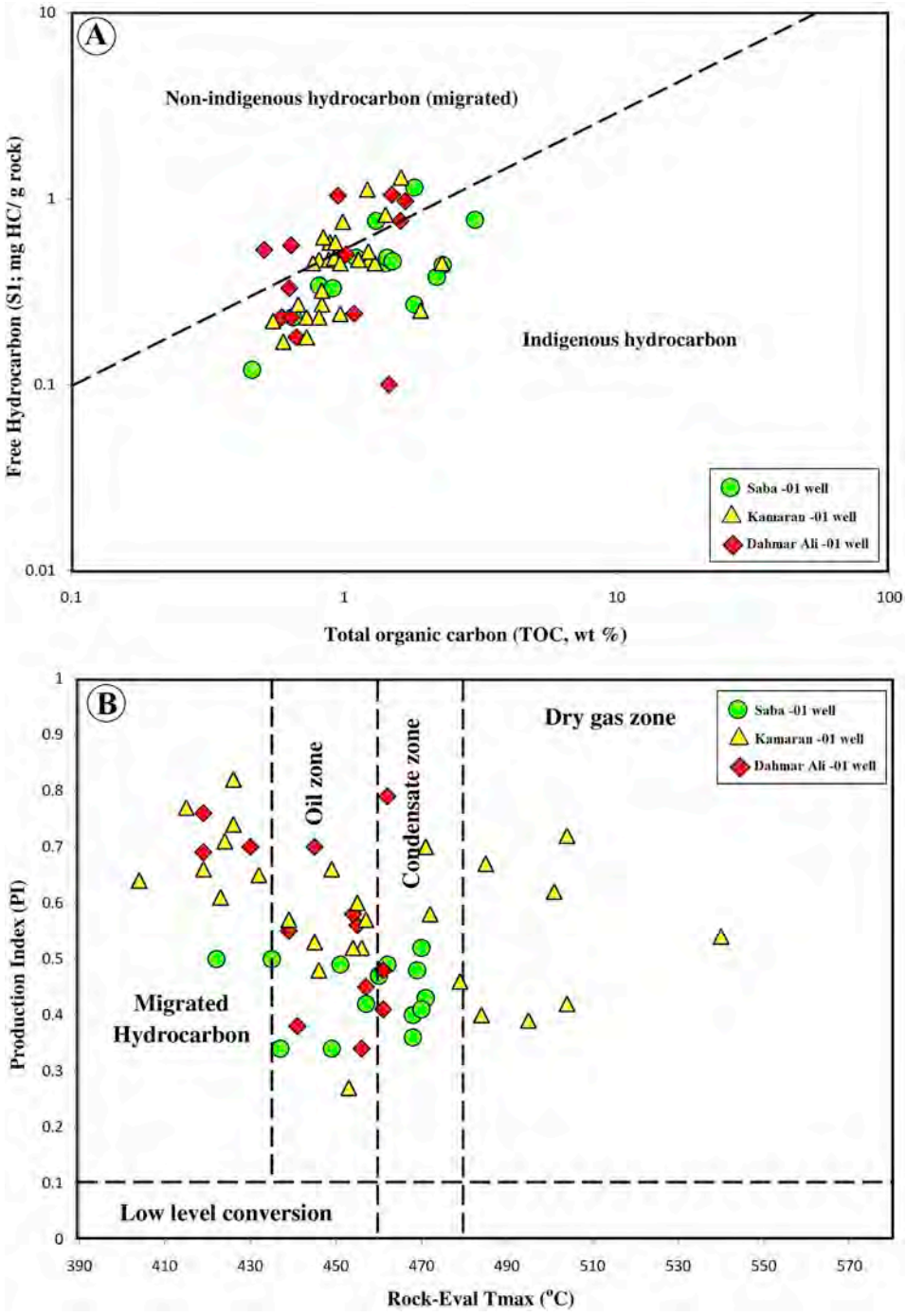

Fig. 7. Cross-plots of relationship between the pyrolysis yields of the analyzed samples such as (A) free hydrocarbon (S_1) versus remaining hydrocarbon yield (S_2). and (B) T_{max} versus production index (PI), indicating that there are migrated hydrocarbons within the analyzed samples due to high thermal maturity levels in the range of mature to over-mature stages.

and based on the calibrated values of measured VR and corrected BHT (Table 3). The secondary cracking of generated oil to gas (wet and dry) is thought to begin at 152 °C and higher, depending on the heating rate (Fig. 14). The secondary cracking process (gas-cracking) of the generated oil from the Arwa source rock reached VR values of between 1.30%Ro and 2.93%Ro (Fig. 15). However, the timing of the oil generation and gas cracking is different among the studied wells. The simulated results for the Dahmar Ali-01 and Kamaran-01 wells show that the oil was generated during the Late Jurassic at approximately 154 to 149 Ma, and that generation continued until the Miocene at 23 Ma in the Kamaran-01 well (Fig. 15A and B). The subsequent thermal maturity of higher than 1.30 %Ro suggests that the generated oil began cracking to gas during the Late Jurassic (149 Ma) and carried on into the Early Miocene (23 Ma); this process has continued until the present-day (Fig. 15A and B). The high thermal maturity level during the Late Jurassic in wells Dahmar Ali-01and Kamaran-01 can be attributed to the significant thickness of the sedimentary rocks deposited during the Late Jurassic-Cretaceous rifting (Redfern and Jones, 1995; As-Saruri et al., 2010), which brought the Arwa shale source rock to depths and temperatures (80–152 °C; Fig. 14) that enabled the generation of

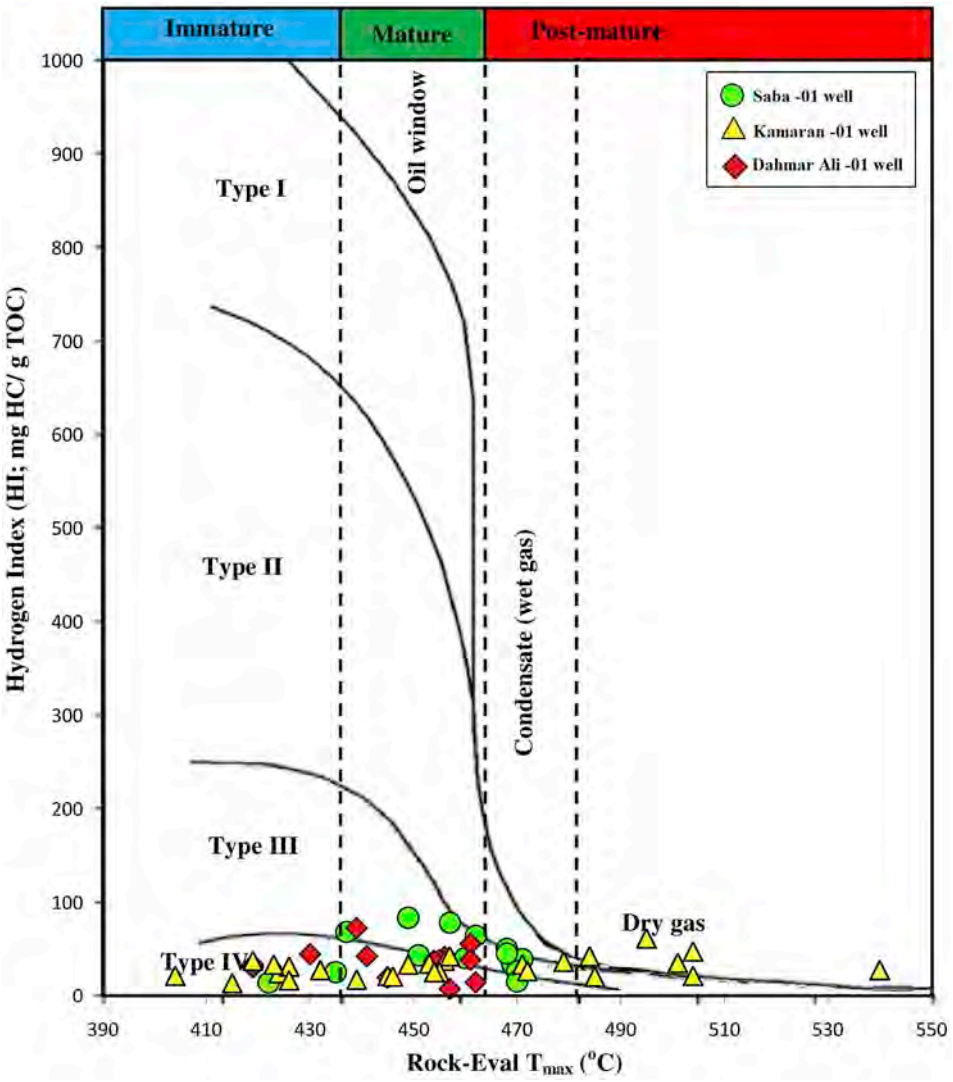

Fig. 8. Pseudo-van Krevelen diagrams of pyrolysis Hydrogen index (HI) versus T_{max}, showing mainly present-day Type types of III and IV kerogen of the analyzed Arwa samples from three studied wells.

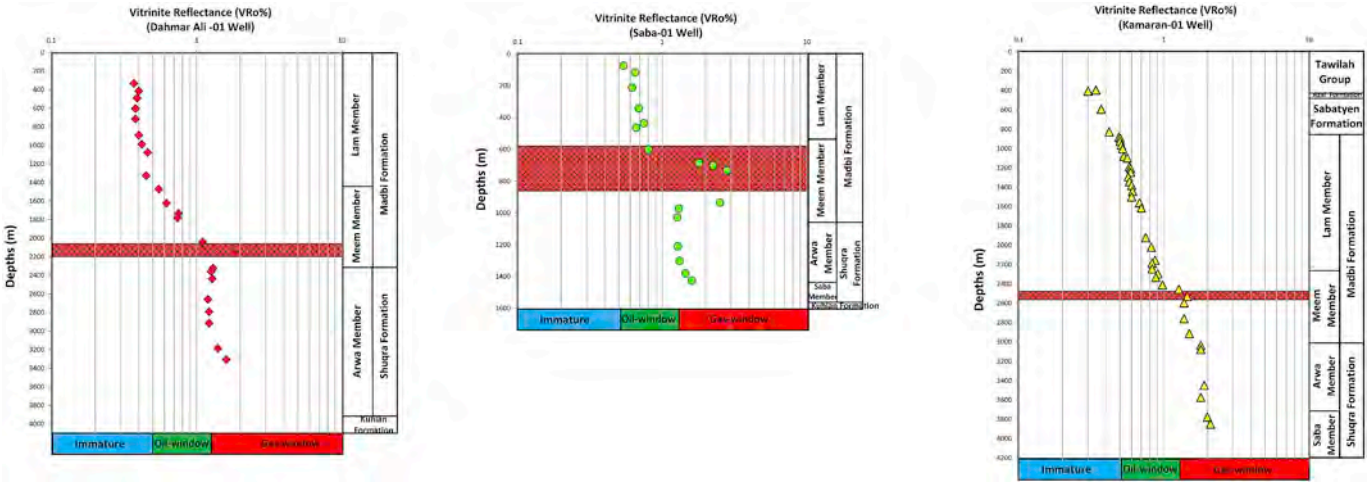

Fig. 9. Plot of vitrinite reflectance measurements adjacent depth, showing thermal maturity trend in the studied wells (Kamaran-01, Dahmar Ali −01 and Saba-01), south-eastern Al-Jawf sub-basin, and showing that the Arwa Member is currently in a gas-window maturity.

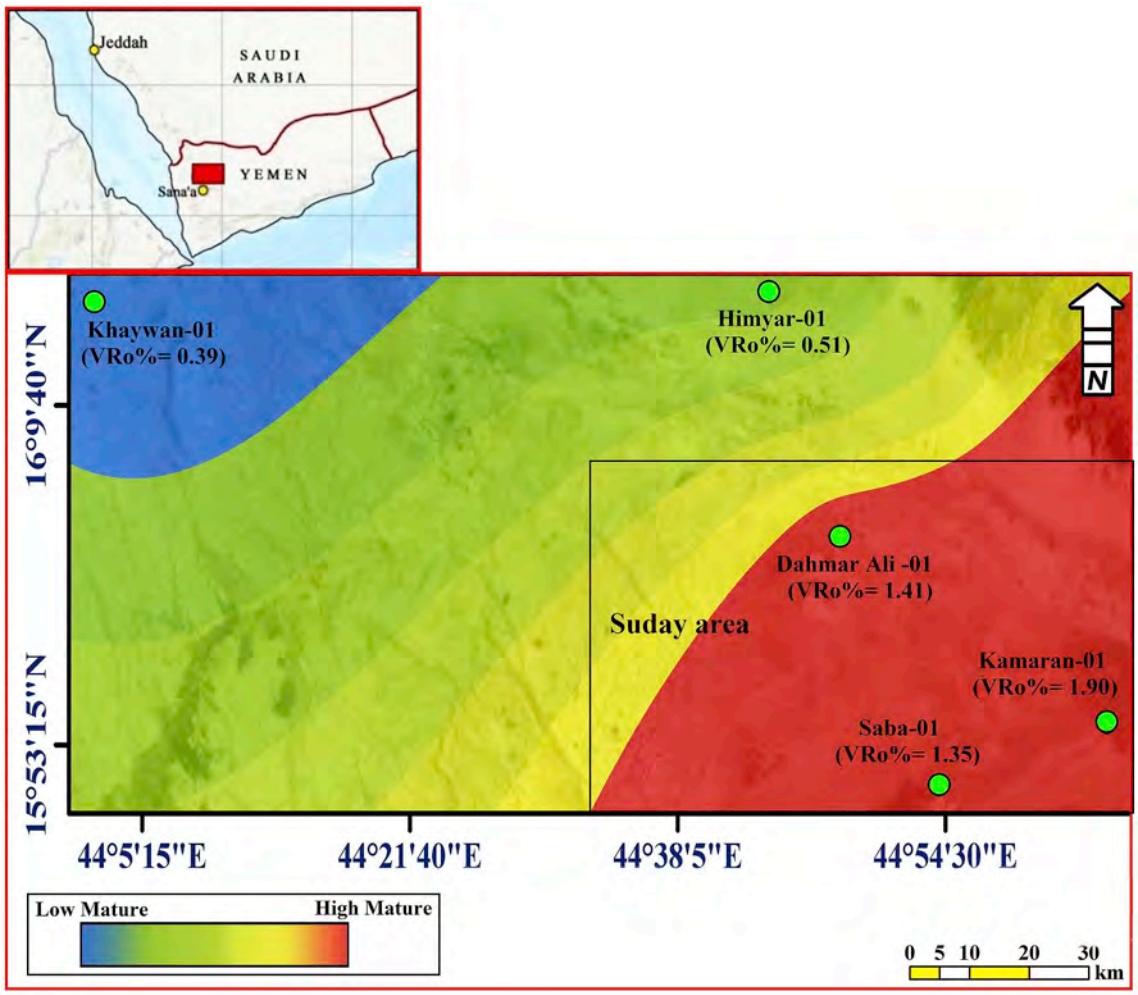

Fig. 10. Map view of thermal maturity levels for the Late Jurassic Arwa Member, using measured vitrinite reflectance data from five wells (Himyar-01 and Khaywan-01, Kamaran-01, Dahmar Ali-01, and Saba-01) along Al-Jawf sub-basin.

petroleum (oil and gas) (Fig. 15). In contrast, the Arwa Member is located at shallow burial depths (1054–1417 m) in the Saba well (Fig. 14C), and its source rock entered the hydrocarbon generation threshold in the Early Miocene at about 20 Ma, and has continued to the present (Fig. 15C). The maturity of the VR distribution range of the current source rock is 0.70 and 1.62 %Ro (Fig. 15C), and regional temperature is in the range of 80–159 °C (Fig. 15C). The high thermal maturity during the Early Miocene was due to the presence of volcanic rocks that formed during the Miocene and have continued to from since then (Mattash, 1994; Al-Kadasi, 1994; Nasher, 2010).

Since the transformation ratios were calculated for the current source rock of the Arwa unit according to the assigned reaction kinetics (Tissot et al., 1987), the amount of oil generated from Type-II kerogen and the oil that cracked to gas were expressed by using oil and gas windows based on computed VR values, as shown in Fig. 15.

Fig. 16 shows the transformation ratios (TR%) for the bottom of the Arwa shale layers over three time periods. Based on kinetic data from Tissot et al. (1987), the modeling results indicate that the organic material of the Arwa Shale source rock in the south-eastern Al-Jawf sub-basin had achieved approximately 50% conversion to oil during the Late Jurassic and into the Early Miocene (Fig. 16). Up to 80% of the organic matter of the Arwa Shale layer was transformed to oil during the Early Miocene within the deepest parts of the Kamaran-01 well (Fig. 16A). Therefore, the Arwa Shale layers generated a higher amount of oil as compared to the Dahmar Ali-01 and Saba-01 wells (Fig. 16). Maximum TRs of 97–99% are thought to have been reached where the generated oils have been trapped or cracked to gas (Fig. 16).

4.6. Exploration aspects— a general outlook

This study intended to provide a general outlook at the expulsion and/or retention of petroleum in sources of shale intervals of the Arwa Member for improving the understanding of the local conventional or unconventional resource systems and aiding petroleum exploration in the Al-Jawf sub-basin, NW Sabatayn.

The results of this study, together with additional geological information concerning the thickness and lithology of the Arwa Member and rifting tectonics, provide evidence that the Arwa Member is a closed system and can be considered as an unconventional resource system (Jarvie et al., 2004).

The Arwa Member system is characterized bya cross-sectional thickness of 363–1593 m (Table 1), and is composed of carbonate rocks and shale interbeds (Fig. 2). The shale intervals in the Arwa Member are an important source of petroleum. The shales have generated oil in the past and currently act as a potential source for shale-gas because of the high level of thermal maturity (Figs. 5–11). The potential for oil and gas generation was simulated numerically for the three wells (Dahmar Ali-0, Saba-01, and Kamaran-01) using the PetroMod1 1D basin modeling

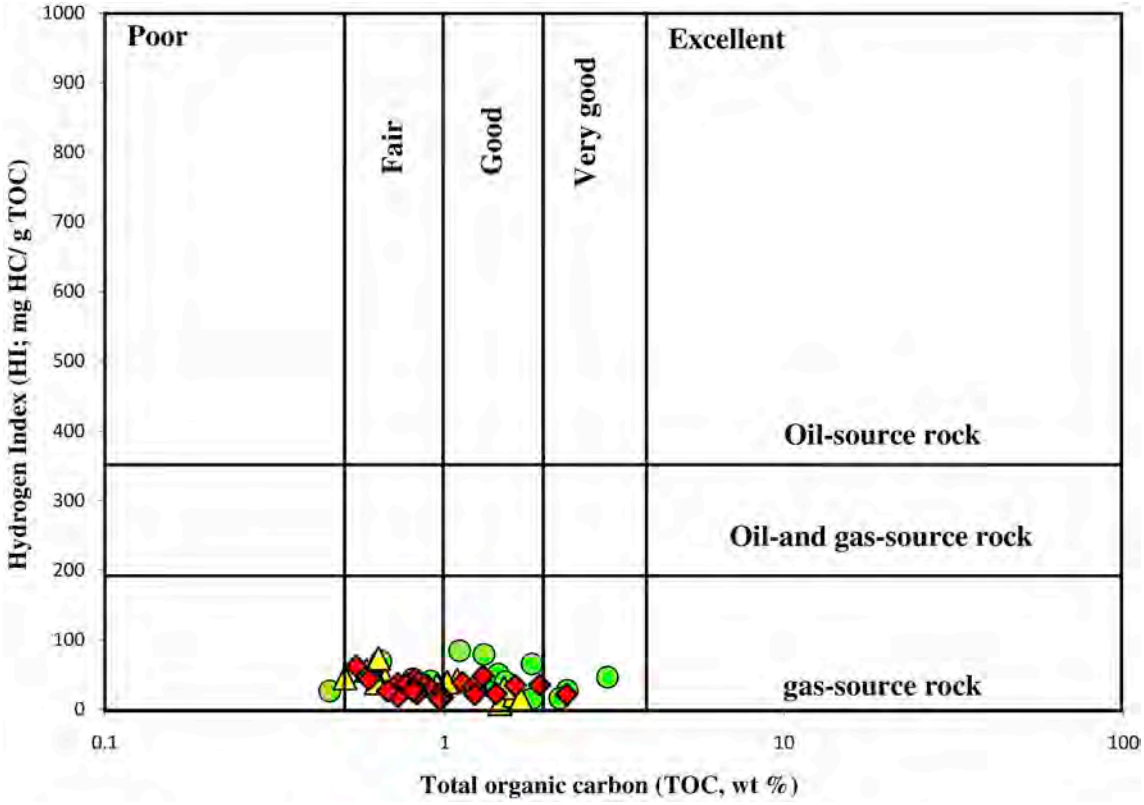

Fig. 11. Relationship between total organic matter (TOC) content and hydrogen index (HI), showing gas generation potential from the analyzed Arwa shale from three studied wells.

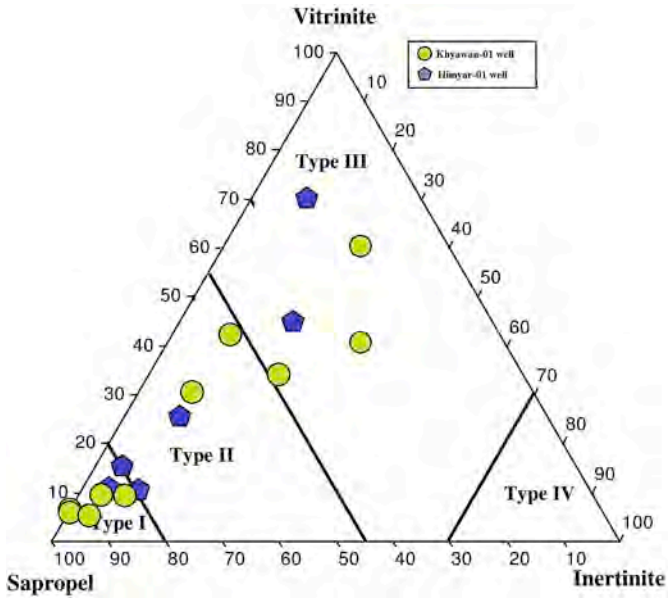

Fig. 12. Ternary plot of the organic matter under microscope for the analyzed shale samples in the two wells (Khyawan-01 and Himyar-01), showing kerogen type (data modified from Hakimi et al., 2018).

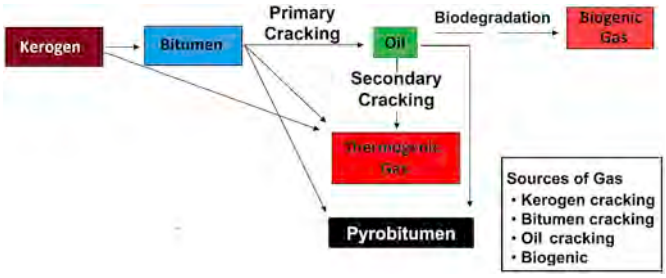

Fig. 13. Processes in a source rock leading to oil, gas, and carbon-rich residue (pyrobitumen). High-maturity shale-gas systems derive high gas contents from the indigenous generation of gas from kerogen, bitumen, and oil cracking (modified after Jarvie et al., 2007).

software (Figs. 14–16). These basin models indicate that the Arwa shale source rock reached a transformation ratio of more than 50% (Fig. 16), a maximum for oil generation that in turn caused high pressures along the Arwa shale source rock, leading to the expulsion of oil. (Hantschel and Kauerauf, 2009). The buildup of pressure due to the presence of maximum oil generation also forms micro-fractures along the shale source rock. The generated oil was expelled through these micro-fractures and retained locally in the carbonate rocks of the Arwa Member, undergoing cracking to gas at temperatures above 150 °C (Fig. 14). At such high temperatures, more thermogenic gas was formed from the secondary cracking of retained oil in the Arwa Member (Fig. 16). This gas was stored as free gas in pore spaces or fractures in the Arwa carbonate rock, created either by diagenetic or rifting tectonic processes during Late Jurassic after the deposition of the Arwa Member. However, further analyses such as mineralogy or diagenetic and petrophysical properties (i.e. porosity and permeability) are recommended to understand the quality of the Arwa carbonate rocks for any future exploration and development in the Al-Jawf sub-basin.

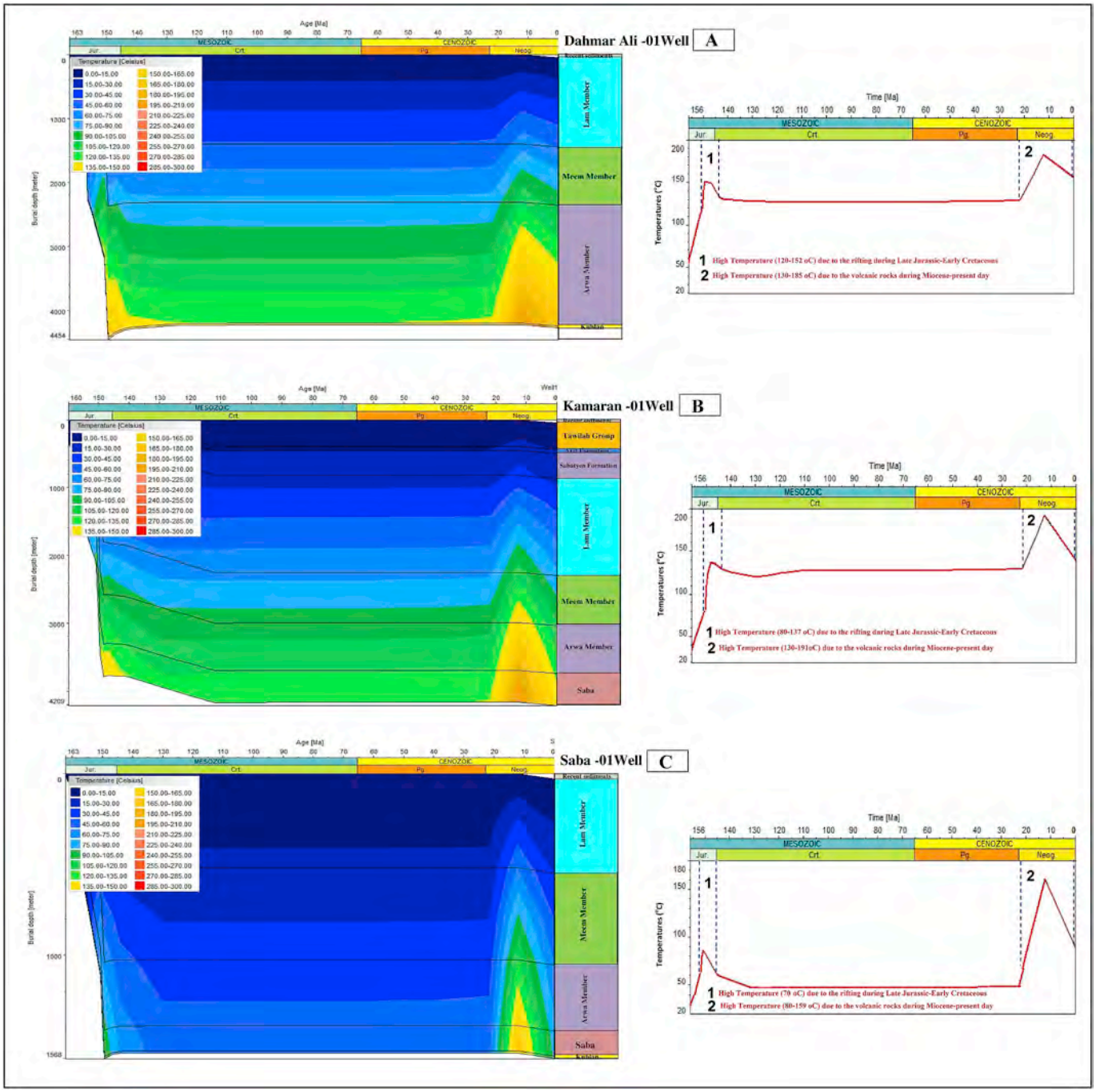

Fig. 14. Left: burial and thermal gradient histories (colored areas) cross all rock units and Right: red lines are shown exclusively for computed temperatures of the Arwa Member in the Dahmar Ali −01, Kamaran-01 and Saba-01 wells, respectively.

5. Conclusions

Source rock geochemical investigation and 1D basin modeling studies were conducted on the Late Jurassic Arwa Member from three wells in the south-eastern Al-Jawf sub-basin, NW Sabatayn Basin. The results of this study reveal that the Arwa Member is a closed source-reservoir system containing shales that are considered as a potential shale-gas source. These results indicate the following:

1 Good source rock potential, with present-day TOC of the shale samples ranging between 0.46% and 3.02% (Mean = 1.14%).
2 The Arwa shales currently consist of Types III and IV kerogen as indicated from their HI values, ranging from 8 to 84 mg HC/g TOC. This indicates the presence of a potential shale-gas source.
3 Integration of maturity data parameters, including VR and pyrolysis (i.e. T_{max} and PI), of the analyzed samples indicates high maturity conditions of the gas-window level. This implies that commercially

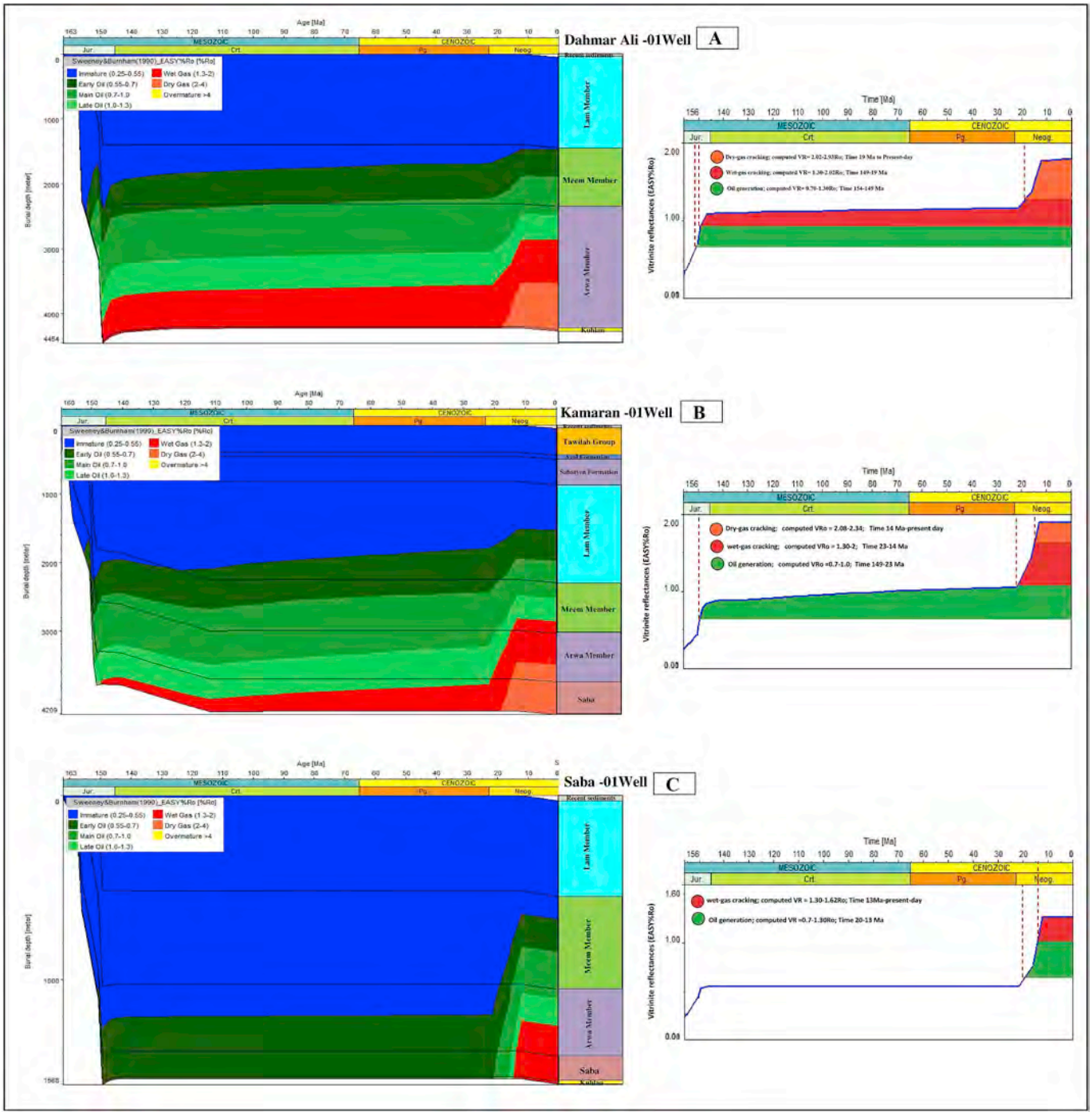

Fig. 15. Left: burial and thermal maturity histories (colored areas) cross all rock units and Right: blue lines are shown exclusively for calculated vitrinite reflectance of the Arwa Member in the in the Dahmar Ali −01, Kamaran-01 and Saba-01 wells, respectively.

viable gas has been generated.

4 Basin models indicate primary and secondary cracking of kerogen and retained oil. The oil was generated during the late Jurassic to early Miocene age, with a kerogen conversion ratio of 10–85 TR%. The large amounts of oil generated during this time caused a pressure buildup along the Arwa Member. It is probable that this pressure formed several micro-fractures.

5 Most of the generated oil was expelled along the micro-fractures and then trapped in the carbonate reservoir rocks within the Arwa Member itself. The retained oil in the Arwa carbonate rocks partially and/or completely cracked between the early Miocene and the present-day and formed thermogenic gas.

6 The results of this study also offer guidance for further gas-generation prospecting and exploration studies that may occur within the Al-Jawf sub-basin.

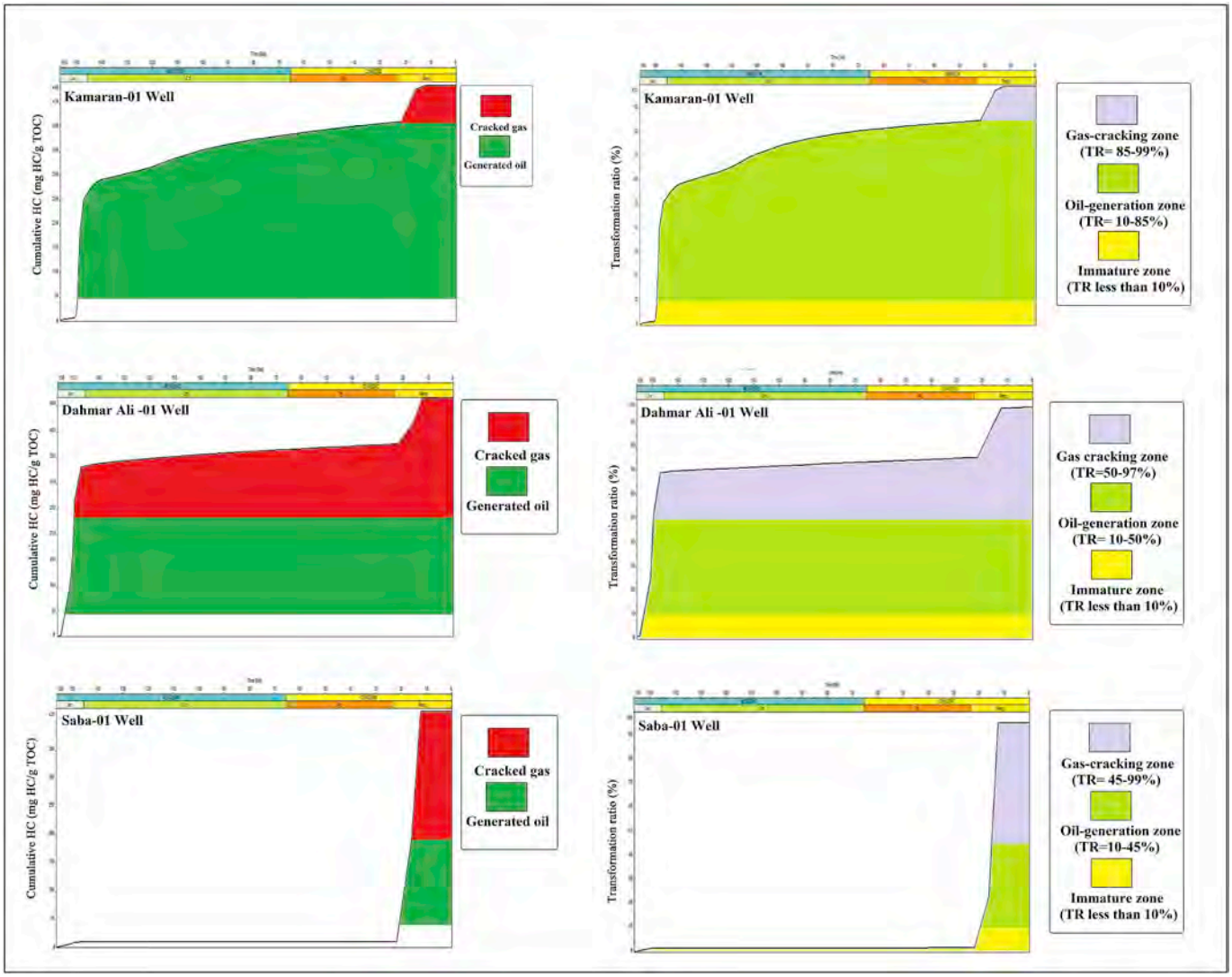

Fig. 16. Left: modelled of cumulative hydrocarbon generation, and Right: Evolution of the transformation ratio with age for the Late Jurassic Arwa shale source rock in the in the Kamaran-01, Dahmar Ali −01 and Saba-01 wells, respectively.

Acknowledgements

The authors are grateful to the Petroleum Exploration and Production Authority (PEPA), the Republic of Yemen for providing the geochemical data used in this study. The provision of a free version of the 1D PetroMod basin modeling software by Schlumberger is also gratefully acknowledged.

References

Abeed, Q., Littke, R., Strozyk, F., Uffmann, A.K., 2013. The Upper Jurassic–Cretaceous petroleum system of southern Iraq: a 3-D basin modelling study. GeoArabia 18, 179–200.

Abrams, M.A., Gong, C., Garnier, C., Sephton, M.A., 2017. A new thermal extraction protocol to evaluate liquid rich unconventional oil in place and in-situ fluid chemistry. Mar. Petrol. Geol. 88, 659–675. https://doi.org/10.1016/j.marpetgeo.2017.09.014.

Alalade, B., Tyson, R.V., 2013. Influence of igneous intrusions on thermal maturity of Late Cretaceous shales in the Tuma-1 well, Chad Basin, NE Nigeria. J. Afr. Earth Sci. 77, 59–66. https://doi.org/10.1016/j.jafrearsci.2012.09.006.

Al-Areeq, N.M., Al-Badani, M.A., Salman, A.H., Albaroot, M., 2018. Petroleum source rocks characterization and hydrocarbon generation of the upper jurassic succession in jabal ayban field, Sabatayn Basin, Yemen. Egypt. J. Petrol. 27, 835–851.

Alaug, A.S., Leythäeuser, D., Bruns, B., Ahmed, A.F., 2011. Source and reservoir rocks of the Block 18 oilfields, Sabatayn Basin, Yemen: source rock evaluation, maturation, and reservoir characterization. Iranian J. Earth Sci. 3, 134–152.

Alaug, A.S., Al-Wosabi, K.A., 2015. Organic geochemical evaluation of Madbi source rock, Al-Jawf basin, NE Central Yemen. Iranian J. Earth Sci. 7, 25–36.

Al-Kadasi, M.A., 1994. Temporal and Spatial Evolution of the Basal Flow of the Yemen Volcanic Group. Ph.D. Thesis. University of London, pp. 284p.

Al-Wosabi, M.A., Al-Mashaikie, S.Z., 2006. Investigation of facies types and associations of Kuhlan Red Bed Formation in NW Yemen: a new hypothesis for origin and depositional environment. SQU J.Sci. 11, 11–38. https://doi.org/10.24200/squjs.vol11iss0pp11-38.

As-Saruri, M.A., Sorkhabi, R., Baraba, R., 2010. Sedimentary basins of Yemen: their tectonic development and lithostratigraphic cover. Arab. J. Geosci. 3, 515–527. https://doi.org/10.1007/s12517-010-0189-z.

Beydoun, Z.R., 1989. The hydrocarbon prospects of the Red Sea-Gulf of Aden: a review. J. Petrol. Geol. 12, 125–144. https://doi.org/10.1111/j.1747-5457.1989.tb00229.x.

Beydoun, Z.R., 1991. Arabian plate hydrocarbon geology and potential—a plate tectonic approach: tulsa, Oklahoma. AAPG Stud. Geol. 33, 1–69.

Beydoun, Z.R., Al-Saruri, M., El-Nakhal, H., Al-Ganad, I.N., Baraba, R.S., Nani, A.S.O., Al-Aawah, M.H., 1998. International lexicon of stratigraphy. In: second ed. International Union of Geological Sciences and Ministry of Oil and Mineral Resources, vol. III. Republic of Yemen, Publication, Republic of Yemen, pp. 245 34.

Bordenave, M.L., 1993. Applied Petroleum Geochemistry. Editions Technip, Paris.

Bosence, D.W.J., 1997. Mesozoic rift basins of Yemen. Mar. Petrol. Geol. 14, 611–616. https://doi.org/10.1016/S0264-8172(97)00039-1.

Brannin, J., Sahota, G., Gerdes, K.D., Berry, J.A.L., 1999. Geological evolution of the central Marib–Shabwah basin. Yemen. GeoArabia 4, 9–34.

Csato, I., Habib, A., Kiss, K., Kocz, I., Kovacs, V., Lorincz, K., Milota, K., 2001. Play concepts of oil exploration in Yemen. Oil Gas J. 99, 68–74.

Espitalie, J., Bordenave, M.L., 1993. Source rock parameters. In: Bordenave, M.L. (Ed.), Applied Petroleum Geochemistry. Technip, Paris, pp. 219–225.

Hadad, Y.T., Hakimi, M.H., Abdullah, W.H., Makeen, Y.M., 2016. Thermal maturity history reconstruction and hydrocarbon generation/expulsion modeling of the syn-rift Rudeis and Kareem source rocks in the Red Sea Rift Basin, Sudan. Arab. J. Geosci

(in press). https://doi.org/10.1007/s12517-016-2458-y.
Hadad, Y.T., Hakimi, M.H., Abdullah, W.H., Makeen, Y.M., 2017. Basin modeling of the late Miocene Zeit source rock in the Sudanese portion of red sea basin: implication for hydrocarbon generation and expulsion history. Mar. Petrol. Geol. 84, 311–322. https://doi.org/10.1016/j.marpetgeo.2017.04.002.
Hakimi, M.H., Abdullah, W.H., 2013a. Organic geochemical characteristics and oil generating potential of the Upper Jurassic Safer shale sediments in the Marib-Shabowah Basin, western Yemen. Org. Geochem. 54, 115–124. https://doi.org/10.1016/j.orggeochem.2012.10.003.
Hakimi, M.H., Abdullah, W.H., 2013b. Geochemical characteristics of some crude oils from Alif Field in the Marib-Shabowah Basin, and source-related types. Mar. Petrol. Geol. 45, 304–314. https://doi.org/10.1016/j.marpetgeo.2013.05.008.
Hakimi, M.H., Abdullah, W.H., 2015. Thermal maturity history and petroleum generation modelling for the Upper Jurassic Madbi source rocks in the Marib-Shabowah Basin, western Yemen. Mar. Petrol. Geol. 59, 202–216. https://doi.org/10.1016/j.marpetgeo.2014.08.002.
Hakimi, M.H., Abdullah, W.H., Shalaby, M.R., 2010. Organic geochemistry, burial history and hydrocarbon generation modeling of the upper Jurassic Madbi formation, Masila basin. Yemen. J. Pet. Geol. 33, 299–318.
Hakimi, M.H., Abdullah, W.H., Shalaby, M.R., Alramisy, G.A., 2014. Geochemistry and organic petrology study of Kimmeridgian organic-rich shales in the Marib-Shabowah Basin, Yemen: origin and implication for depositional environments and oil-generation potential. Mar. Petrol. Geol. 50, 185–201. https://doi.org/10.1016/j.marpetgeo.2013.09.012.
Hakimi, M.H., Nasher, M.A., Saeed, S.A., Al-Hakame, H., Al-Moliki, T., Al-Sharabi, K.Q., 2017. Metamorphosis of marine organic matter in the jurassic deposits from sharab area, taiz governorate of southwestern Yemen: thermal effect of tertiary volcanic rocks. J. Geol. Soc. India 89, 325–330. https://doi.org/10.1007/s12594-017-0607-x.
Hakimi, M.H., Alaug, A.S., Ahmed, A.F., Yahya, M.M.A., 2019. Sedimentary environmental conditions and petroleum source rock potential of the Late Jurassic Arwa Member shales in Al-Jawf sub-basin. Yemen. J. Afric. Earth Sci. 149, 474–486.
Hantschel, T., Kauerauf, A.I., 2009. Fundamentals of Basin and Petroleum Systems Modeling: Integrated Exploration Systems GmbH. Schlumberger Company. Springer-Verlag Berlin Heidelberg. https://doi.org/10.1007/978-3-540-72318-9.
Hatem, B.A., Abdullah, W.H., Hakimi, M.H., Mustapha, K.A., 2016. Origin of organic matter and paleoenvironmental conditions of the Late Jurassic organic-rich shales from Shabwah sub-basin (Western Yemen): constraints from petrology and geochemical proxies. Mar. Petrol. Geol. 72, 83–97.
Huang, W.H., Ao, W.H., Weng, C.M., 2010. Characteristics of coal petrology and genesis of Jurassic coal in Ordos Basin. Geoscience 24 1186–1120.
Hunt, J.M., 1996. Petroleum Geochemistry and Geology, second ed. W. H. Freeman and Company, New York.
Jarvie, D.M., Hill, R.J., Pollastro, R.M., 2004. Assessment of the gas potential and yields from shales: the Barnett Shale model. Okla. Geol. Surv. Circ. 110, 37–50.
Jarvie, D.M., Hill, R.J., Ruble, T.E., Pollastro, R.M., 2007. Unconventional shale-gas-systems: the Mississippian Barnett Shale of north-central Texas as one model for thermogenic shale-gas assessment. AAPG (Am. Assoc. Pet. Geol.) Bull. 91, 475–499. https://doi.org/10.1306/12190606068.
Jones, R.W., 1984. Comparison of carbonate and shale source rocks. In: In: Palacas, J. (Ed.), Petroleum Geochemistry and Source Rock Potential of Carbonate Rocks, vol. 18. AAPG Stud.Geol., pp. 163–180.
Killops, S.D., Killops, V.J., 2005. Introduction to Organic Geochemistry, second ed. Blackwell Publishing Limited. https://doi.org/10.1002/9781118697214.
Lewan, M.D., Henry, A.A., 2001. Gas: oil ratios for source rocks containing Type-I, -II, -IIS, and -III kerogens as determined by hydrous pyrolysis. In: Dyman, T.S., Kuuskraa, V.A. (Eds.), Geologic Studies of Deep Natural Gas Resources. U.S. Geological Survey.
Liu, J., Qin, Z., Zhang, P., 2015. Evaluation of hydrocarbon source rocks and oil source analysis of dense reservoir in Malang sag. Special Oil Gas Reservoirs 22, 35–39.
Makeen, Y.M., Abdullah, W.H., Pearson, M.J., Hakimi, M.H., Elhassan, O.M.A., Hadad, Y.T., 2016. Thermal maturity history and petroleum generation modelling for the lower Cretaceous Abu Gabra Formation in the Fula sub-basin, Muglad basin, Sudan. Mar. Petrol. Geol. 75, 310–324. https://doi.org/10.1016/j.marpetgeo.2016.04.023.
Manning, D.A.C., 1991. Organic Geochemistry: Advances and Applications in the Natural Environment. Manchester University Press, Manchester.
Mattash, M.A., 1994. Study of the Cenozoic Volcanics and their associated intrusive rocks in Yemen in relation to rift development. Ph.D. Thesis In: Hungarian Acad. Sci. Eötvös Loránd Univ., Budapest, pp. 112.
Nasher, M.A., 2010. Geology and Geochemistry of the Tertiary Volcanic Rocks and Their Allied Intrusion at NW Ad-Dhala Province, Yemen. PhD Thesis. Cairo Univ., Egypt, pp. 250.
Peters, K.E., 1986. Guidelines for evaluating petroleum source rock using programmed pyrolysis. Am. Assoc. Petrol. Geol. Bull. 70, 318–329.
Peters, K., Cassa, M., 1994. Applied source rock geochemistry. In: Magoon, L.B., Dow, W.G. (Eds.), 1994, the Petroleum System from Source to Trap. vol. 60. AAPG Memoir, pp. 93–117.
Redfern, P., Jones, J.A., 1995. The interior rifts of Yemen–701 analysis of basin structure and stratigraphy in a regional plate tectonic context. Basin Res. 7, 337–356.
Sachsenhofer, R.F., Bechtel, A., Dellmour, R.W., Mobarakabad, A.F., Gratzer, R., Salman, A., 2012. Upper Jurassic source rocks in the Sab'atayn Basin, Yemen: depositional environment, source potential and hydrocarbon generation. GeoArabia 17, 161–186.
Shalaby, M.R., Hakimi, M.H., Abdullah, W.H., 2011. Geochemical characteristics and hydrocarbon generation modeling of the Jurassic source rocks in the Shoushan Basin, north Western Desert, Egypt. Mar. Petrol. Geol. 28, 1611–1624. https://doi.org/10.1016/j.marpetgeo.2011.07.003.
Shalaby, M.R., Hakimi, M.H., Abdullah, W.H., 2012. Geochemical characterization of solid bitumen (migrabitumen) in the Jurassic sandstone reservoir of the Tut field, Shushan basin, northern Western desert of Egypt. Int. J. Coal Geol. 100, 26–39. https://doi.org/10.1016/j.coal.2012.06.001.
Shalaby, M.R., Hakimi, M.H., Abdullah, W.H., 2013. Modeling of gas generation from the Alam El-Bueib Formation in the shoushan basin, northern western desert of Egypt. Int. J. Earth Sci. 102, 319–332. https://doi.org/10.1007/s00531-012-0793-0.
SPT, 1994. The Petroleum Geology of the Sedimentary Basins of the Republic of Yemen, vols. 1–7 Unpublished Report.
Sweeney, J.J., Burnham, A.K., 1990. Evaluation of a simple model of vitrinite reflectance based on chemical kinetics. Am. Assoc. Petrol. Geol. Bull. 74, 1559–1570.
Teichmüller, M., Littke, R., Robert, P., 1998. Coalification and maturation. In: Taylor, G.H., Teichmüller, M., Davis, A., Diessel, C.F., Littke, R., Robert, P. (Eds.), Organic Petrology. Gebrüder Borntraeger, Berlin, pp. 86e174.
Tissot, B.P., Welte, D.H., 1984. second ed. Petroleum Formation and Occurrence Springer Verlag, Berlin, pp. 699. https://doi.org/10.1007/978-3-642-87813-8.
Tissot, B.P., Pelet, P., Ungerer, R., 1987. Thermal history of sedimentary basins, maturation indices, and kinetics of oil and gas generation. Am. Assoc. Petrol. Geol. Bull. 71, 1445–1466.
Zhang, X., 2012. The evaluation of the source rocks and the oil source comparison of the 15 well source rocks. Inner Mongolia Petrochem. Indus. 14, 127–128.
Zhu, D., Jin, Z., Hu, W., Song, Y., Gao, X., 2007. Effect of igneous activity on hydrocarbon source rocks in Jiyang sub-basin, eastern China. J. Petrol. Sci. Eng. 59, 309–320. https://doi.org/10.1016/j.petrol.2007.05.002.